Deletion of Stk11 and Fos in mouse BLA projection neurons alters intrinsic excitability and impairs formation of long-term aversive memory

Abbreviated Title: The role of Stk11 in memory formation

David Levitan[2]*, Chenghao Liu[2]*, Tracy Yang[2], Yasuyuki Shima[2], Jian-You Lin[1, 3], Joseph Wachutka[1], Yasmin Marrero[1], Ramin Ali Marandi Ghoddousi[2], Eduardo da Veiga Beltrame[1], Donald B. Katz[1, 3], Sacha B. Nelson[2, 3]

Departments of Psychology[1], Biology[2], and Volen Center for Complex Systems[3], Brandeis University, Waltham, Massachusetts 02454, USA.

*D.L. and C.L. contributed equally

Proofs and correspondence to:

Sacha B Nelson, MD, PhD, Brandeis University

Department of Biology, MS 062, 415 South Street, Waltham, MA 02454,

Email: nelson@brandeis.edu

Declaration of Interest: The authors declare no competing financial interests.
Acknowledgements: This research was supported by the National Institute on Deafness and Other Communication Disorders (NIDCD) DC006666 and by NINDS NS109916.

Abstract

Conditioned taste aversion (CTA) is a form of one-trial learning dependent on basolateral amygdala projection neurons (BLApn). Its underlying cellular and molecular mechanisms are poorly understood, however. We used RNAseq from BLApn to identify learning-related changes in Stk11, a kinase with well-studied roles in growth, metabolism and development, but not previously implicated in learning. Deletion of Stk11 restricted to BLApn completely blocks memory when occurring prior to training, but not following it, despite altering neither BLApn-dependent encoding of taste palatability in gustatory cortex, nor transcriptional activation of BLApn during training. Deletion of Stk11 in BLApn also increases their intrinsic excitability. Conversely, BLApn activated by CTA to express the immediate early gene Fos had reduced excitability. BLApn knockout of Fos also increased excitability and impaired learning. These data suggest that Stk11 and Fos expression play key roles in CTA long-term memory formation, perhaps by modulating the intrinsic excitability of BLApn.

Introduction

Conditioned Taste Aversion (CTA) is a form of long-lasting aversive memory induced by a single pairing of exposure to an initially palatable taste with gastric malaise (Bures et al., 1998). Although multiple brain regions, including the brainstem, amygdala and the cortex, participate in various aspects of taste behavior (reviewed in Carleton et al., 2010), prior work suggests that the basolateral amygdala (BLA) plays a critical role in CTA memory. Disrupting neuronal activity within the BLA blocks the formation and retrieval of CTA memory (Yasoshima et al., 2000; Ferreira et al., 2005; Garcia-Delatorre et al., 2014; Molero-Chamizo, et al., 2017). This may reflect the fact that BLA projection neurons (BLApn) provide the principal output pathway from the amygdala to forebrain structures including the gustatory cortex and the central amygdala (Duvarci and Pare, 2014) enabling it to distribute taste valance information to these regions (Piette et al., 2012; Samuelsen et al., 2012). Consistent with this view, BLA neurons change their activity and their functional connectivity with their down-stream targets during CTA learning (Grossman et al., 2008). However, whether the BLA is a site of cellular and molecular plasticity during CTA learning, as opposed to merely gating plasticity in other structures, is not known.

Stages of memory formation are typically distinguished on the basis of duration and molecular mechanism. Short-term memory, lasting minutes to hours, requires only post-translational modification of preexisting proteins, whereas long-term memory, lasting days or longer, requires gene transcription and RNA translation, typically occurring in the hours following memory acquisition (Matthies, 1989; Alberini, 2009; Gal-Ben-Ari et al., 2012; Kandel, 2001). Production of new proteins is required to produce lasting changes in the efficacy of synaptic connections and in the intrinsic excitability of neurons, which are thought to be the cellular correlates of memory (Zhang and Linden, 2003; Mozzachiodi and Byrne, 2010; Takeuchi et al., 2014). The cellular correlates of CTA

learning are less completely understood than those of some other forms of learning, but the involvement of both synaptic plasticity (Li et al., 2016) and intrinsic plasticity (Yasoshima and Yamamoto, 1998; Zhou et al., 2009) have been demonstrated. CTA is known to require protein synthesis in the BLA (Josselyn et al., 2004) and to increase the expression of the activity dependent transcription factor Fos (Uematsu et al., 2015). In other behavioral paradigms, neurons increasing Fos protein undergo changes in synaptic strength and intrinsic excitability (Yassin et al., 2010; Ryan et al., 2015; Pignatelli et al., 2019) and are thought to be essential parts of the neuronal network underlying long-term memory (Tonegawa et al., 2015). However, the role of neurons expressing Fos in the BLA during CTA is unclear. Also unknown is whether CTA learning requires new transcription, and if so, the identities of the required transcripts and cellular processes they promote are not known.

In this study we found that new transcription in the BLA is required for CTA learning. Using RNA-seq from sorted neurons, we found that expression of the kinase Stk11, also known as LKB1, is altered following learning in BLA projection neurons (BLApn), but not in excitatory or inhibitory neurons within the GC. Stk11 is known to act as a master regulator of growth, metabolism, survival and polarity by phosphorylating 13 down-stream members of the AMP-related kinase family (Lizcano et al., 2004; Shackelford and Shaw, 2009). Recent work also suggests roles for Stk11 in the nervous system, where it controls axonal specification and dynamics during development (Barnes et al., 2007; Shelly et al., 2007) and synaptic remodeling during old age (Samuel et al., 2014). Stk11 can also regulate synaptic transmission in forebrain neurons (Kwon et al., 2016), but it is not known to play a role in learning or in the regulation of intrinsic neuronal excitability.

We find that Stk11 is required for CTA since conditional knockout from BLApn prior to training completely blocks learning. However, the same deletion performed two days after training—i.e., at a time when long-term memories have already been formed and stabilized—has no effect on subsequent memory retrieval. Deletion of Stk11 also increased the excitability of BLApn, but did not alter the ability of the BLA-GC circuit to become transcriptionally activated by training or to encode the palatability of gustatory stimuli. CTA training is associated with an opposing decrease in intrinsic excitability change in a sub-population of BLA projection neurons expressing the activity dependent gene Fos following learning. BLApn knockout of Fos also increased excitability and impaired learning. Together, these data suggest that Stk11 and Fos expression play key roles in CTA long-term memory formation, perhaps by modulating the intrinsic excitability of BLApn.

Results

CTA long-term memory requires BLA transcription

In order to determine whether CTA requires new RNA transcription within the BLA, we inhibited transcription by injecting Actinomycin-D (1 µl, 50 ng, bilaterally, Figure 1), a

widely used RNA polymerase 2 inhibitor (Alberini, 2009), into the BLA 20 min prior to CTA training, and tested memory 48 hours later. As a control, a separate group of mice received vehicle injection (1 µl of PBS, bilaterally). CTA training consisted of 30 min of access to 0.5% saccharin followed by an intraperitoneal injection of 0.15M LiCl, 2% body weight; (Figure 1-figure supplement 1). A two-way ANOVA comparing vehicle and

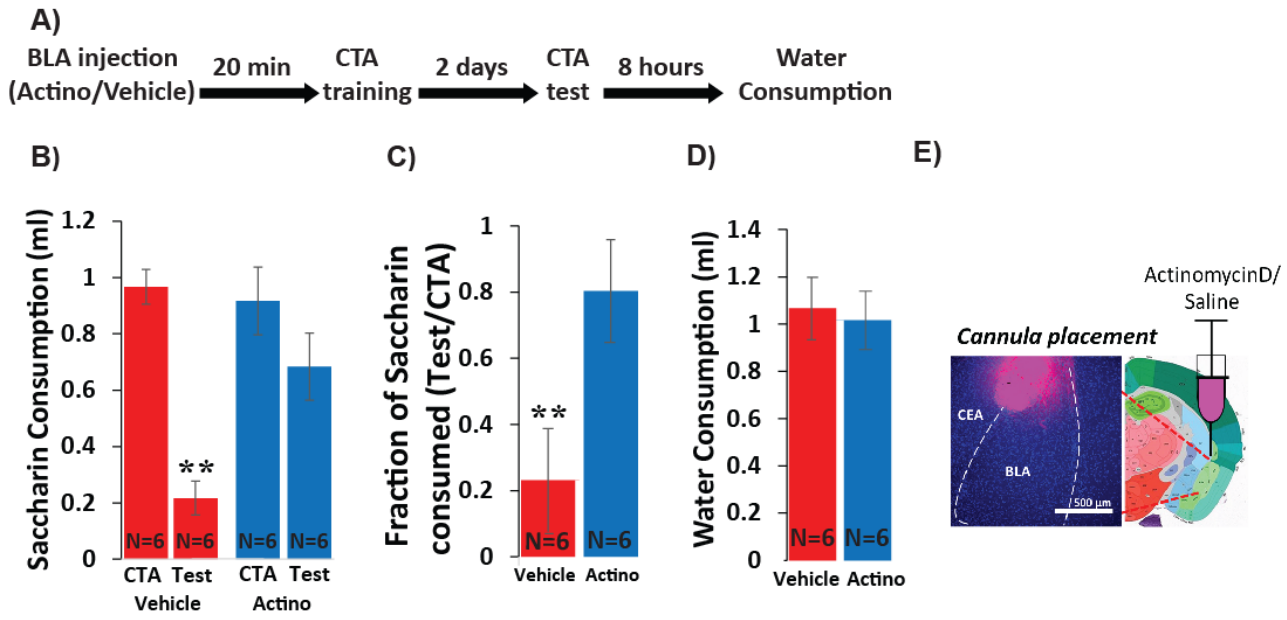

actinomycin-D injected mice before and after training revealed significant training and

Figure 1. Inhibiting BLA transcription impairs CTA Learning. (**A**) Protocol for injection (1 µl per hemisphere) of Actinomycin-D (50 ng) or vehicle (PBS with 0.02% DMSO). (**B**) Actinomycin D injection prior to CTA training impairs learning, expressed as a reduction in saccharin consumption between CTA and test sessions. Group and treatment effects were significant by two-way ANOVA (groups: $F(3,20)=13.05$; $p=6E-5$; treatment: $F(1,20)=4.83$; $p=0.04$; with a significant interaction: $F(1,20)=7.4$; $p=0.013$). Post hoc analysis (Bonferroni corrected) revealed significant reductions ($p=1E-4$) of saccharin consumption (training vs. test for vehicle treated, but not for actinomycin-D treated mice ($p=0.583$). (**C**) Fraction of saccharin consumed (Test/CTA) was significantly higher ($t(10)=-3.36$; $p=0.007$) following Actinomycin D treatment than vehicle, consistent with weaker memory. (**D**) Treatments did not differ in water consumption measured 8 hours later ($t(10)=0.279$; $p=0.794$) suggesting this does not account for differences in consumption during the test. **$p<0.01$. (**E**) Guide cannula was coated with fluorescent dye to assess placement (Left) relative to desired location in anterior BLA (Right; bregma -1.4 mm; Allen brain atlas). Note that the injection cannula extended 0.5 mm further into the BLA.

treatment effects and a significant interaction between the two (Figure 1B), and post-hoc analysis revealed significant reduction in the consumption of saccharin (CTA vs. Test) for the vehicle group, indicating impairment of learning for the actinomycin-D treated group compared to control mice. As a convergent measure, we also assessed the strength of CTA memory by calculating the relative consumption of saccharin during the test day to that consumed on the training day (Neseliler et al., 2011). The differences between the groups were large (23% in the vehicle group vs. 80 % for the actinomycin D group) and

significant. Meanwhile, actinomycin-treated mice were neither impaired in their ability to detect the palatability of saccharin, nor in their drinking behavior—consumption of saccharin during CTA training was similar for the two groups, as was consumption of water 8 hours after the test (Figure 1E), suggesting that these nonspecific effects cannot account for the memory impairment. Thus, BLA transcription is essential for CTA memory formation. These results extend prior work showing the importance of BLA protein synthesis for CTA memory (Josselyn et al., 2004) and together show that training induces both transcription and translation important for CTA in the BLA.

Stk11 expression is regulated in BLA projection neurons following CTA

In order to identify specific transcripts that might be necessary for CTA learning within the BLA, we used cell type-specific RNA-seq to profile transcriptional changes in sorted BLA projection neurons (BLApn). We manually isolated fluorescently labeled BLApn neurons from YFP-H mice (Feng et al., 2000) in which YFP is expressed under the Thy1 promoter in a large population of excitatory projection neurons located in the anterior part of the nucleus (Sugino et al., 2006; Jasnow et al., 2013; McCullough et al., 2016). RNA sequencing was performed separately on YFP^+ BLApn harvested 4 hours following training from mice undergoing CTA, and from taste-only controls (n=4/group) (Figure 2 and Table 1). Sequencing results (Figure 2A) also confirmed the purity and molecular identity of YFP-H neurons in the BLA, as transcripts known to be expressed in BLApn and other forebrain excitatory projection neurons were enriched and transcripts known to be expressed in inhibitory interneurons, glia cells and other neurons in the vicinity of the BLA (lateral amygdala or central amygdala) were virtually absent. Moreover, this observed pattern of expression was comparable to that reported in other studies profiling the same population (Sugino et al., 2006; McCullough et al., 2016).

CTA training changed expression of many genes. Table 1 lists the 20 transcripts showing differential expression between CTA and taste control group based on robust expression criteria: $2 \leq$ fold change ≤ 0.5, $p<0.01$ (unpaired t-test), transcripts-per-million (TPM) ≥ 30. Included among these transcripts is the activity dependent transcription factor, Fos which has previously been shown to be upregulated in BLApn following CTA and other learning paradigms (Zhang et al., 2002; Yasoshima et al., 2006; Mayford and Reijmers. 2015; Uematsu et al. 2015). Our screen for differentially expressed genes also identified Stk11 (also known as LKB1; Figure 2B) a kinase well studied in the context of cancer, cell growth and development, but not previously known to be involved in learning and neuronal plasticity (Bardeesy et al., 2002; Alessi et al., 2006; Barnes et al., 2007; Gurumurthy et al., 2010; Courchet et al., 2013). Changes in the expression of both Fos and Stk11 were validated by qPCR in separate experiments, which revealed a 4.6-fold increase in Fos mRNA ($t(6)=2.5$; $p=0.045$) and a 1.9-fold decrease in Stk11 ($t(6)=-2.5$; $p=0.046$) (Figure 2C). To further examine the significance of these transcriptional changes we also analyzed the levels of Fos and Stk11 protein in the BLA. Due to the availability of antibodies to Fos suitable for immunohistochemistry, we measured the

fraction of Fos-expressing YFP-H neurons in the BLA 4 hours following CTA and found a significant increase relative to lithium chloride-only and taste-only control groups (Figure 2-figure supplement 1). Lacking an antibody to Stk11 usable for immunostaining of brain sections, we examined Stk11 protein 4 hours following CTA and taste control conditions

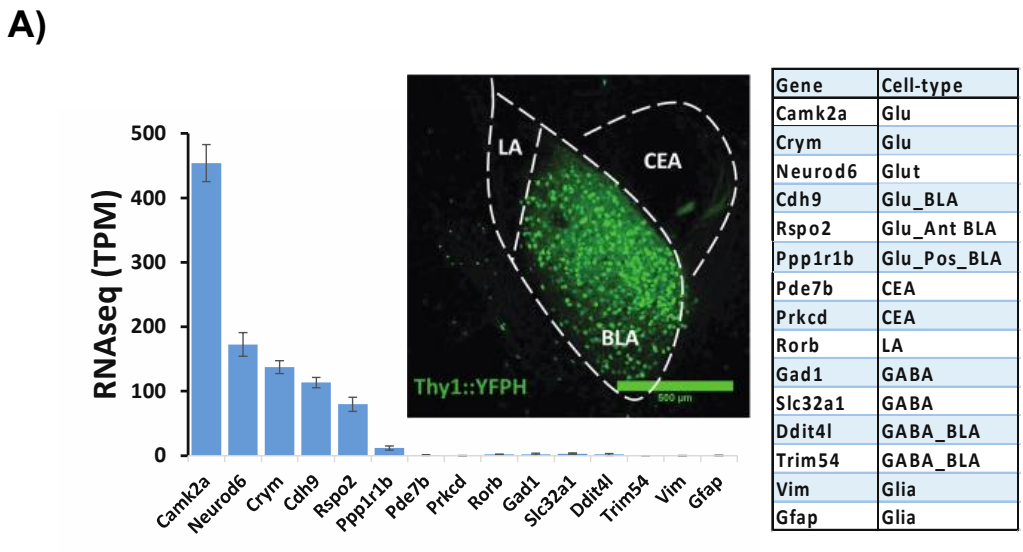

Gene	Cell-type
Camk2a	Glu
Crym	Glu
Neurod6	Glut
Cdh9	Glu_BLA
Rspo2	Glu_Ant BLA
Ppp1r1b	Glu_Pos_BLA
Pde7b	CEA
Prkcd	CEA
Rorb	LA
Gad1	GABA
Slc32a1	GABA
Ddit4l	GABA_BLA
Trim54	GABA_BLA
Vim	Glia
Gfap	Glia

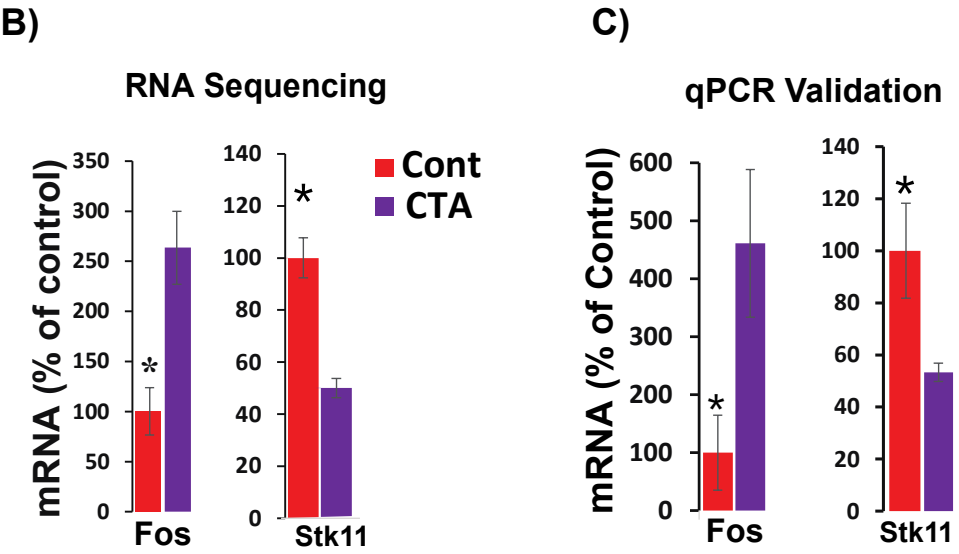

Figure 2. RNA sequencing from BLApn 4 hours following CTA training. (**A**) BLApn were isolated from YFP-H mice following CTA or taste control (N=4/group). Neurons (150-200) were manually sorted form coronal slices (LA-lateral amygdala; CEA-central amygdala). Abundant transcripts (histogram, averaged across both groups) are enriched for those expected in the population and depleted for those expressed in other nearby populations (table) including GABAergic interneurons, glia, neurons in LA or CEA; Sugino et al., 2006; Kim et al., 2016; Allen brain atlas). Glu- GABA-, glutamatergic, GABAergic neurons; AntBLA, PostBLA- Anterior and posterior portions of the BLA. TPM- transcript per million. (**B**) Among genes meeting robust criteria for differential expression (see table 1) Stk11 and Fos were selected for further analysis, including qPCR confirmation (**C)** in separate experiments (N=4/group; *p<0.05).

using immunoblotting of proteins isolated from the anterior BLA. Surprisingly, we found a 1.8- fold increase in Stk11 protein (Figure 2-figure supplement 2). This confirms the fact that Stk11 expression is altered following CTA, but suggests complexity in the dynamics of the expression and potential mismatch in the timing or magnitude of changes in transcript and protein.

Stk11 is at the apex of the AMP-related kinase pathway and mediates its effects by phosphorylating one or more of 13 different downstream kinases, all of which share some homology with AMP-kinase (Lizcano et al., 2004; Shackelford and Shaw. 2009). Among these, YFP^+ BLApn had moderate expression of Brsk2 (TPM=39.9) and Mark2/3 (TPM=59.3 and 73.7 respectively; Figure 2-figure supplement 3), which have known roles in establishing cell polarity during neuronal development (Barnes et al., 2007; Shackelford and Shaw. 2009). Expression of AMP kinase itself (Prkaa1/2), an important metabolic regulator in many cell types (Shackelford and Shaw. 2009) was lower (TPM=16.4 and 22.3 respectively). Comparing kinase expression between CTA and control groups revealed nearly two-fold less expression of Mark2 following CTA (fold-change=0.41; p=0.04, unpaired t-test; data not shown) but this was not significant after Bonferroni correction across the compared kinases.

We also analyzed the impact of CTA on the transcriptional profile of layer 5 pyramidal neurons labeled in strain YFP-H and Pvalb-expressing inhibitory interneurons in the GC, a brain region in which transcription is also known to be important for CTA learning (Imberg et al., 2016). RNA sequencing was performed on YFP^+ and Pvalb+ neurons in the GC harvested from mice 4 hours following CTA training, and from taste-only controls (n=3/4/group). Table 2 and 3 lists the transcripts showing the most differentially expressed genes using the same criteria used in the BLA: $2 \leq$ fold change ≤ 0.5, $p<0.01$ (unpaired t-test), transcripts-per-million (TPM) ≥ 30. While Pvalb+ neurons showed a robust transcriptional response, evident by 19 genes reaching the criteria, only one gene reached the same criteria in YFP+, suggesting a weaker CTA-driven transcriptional response in these neurons. Importantly, the expression of Fos and Stk11 in both YFP+ and Pvalb+ neurons, did not differ between CTA and control groups (Figure 2-figure supplement 4 and Table 2 and 3). This data suggest that the differential expression of Fos and Stk11 during CTA learning may be specific to a subset of cell-types within the circuit.

Fos and Stk11 expression in BLA projection neurons are necessary for memory formation

We next wished to determine whether any of the transcriptional changes in BLApns that correlate with learning are indeed necessary for learning to occur. Since both Fos and Stk11 protein increase following CTA, we pursued a loss of function (LOF) strategy. To restrict LOF to BLApns, we performed conditional deletion by injecting Cre recombinase into mice carrying alleles of Fos (Zhang et al., 2002) or Stk11(Nakada et al., 2010) in

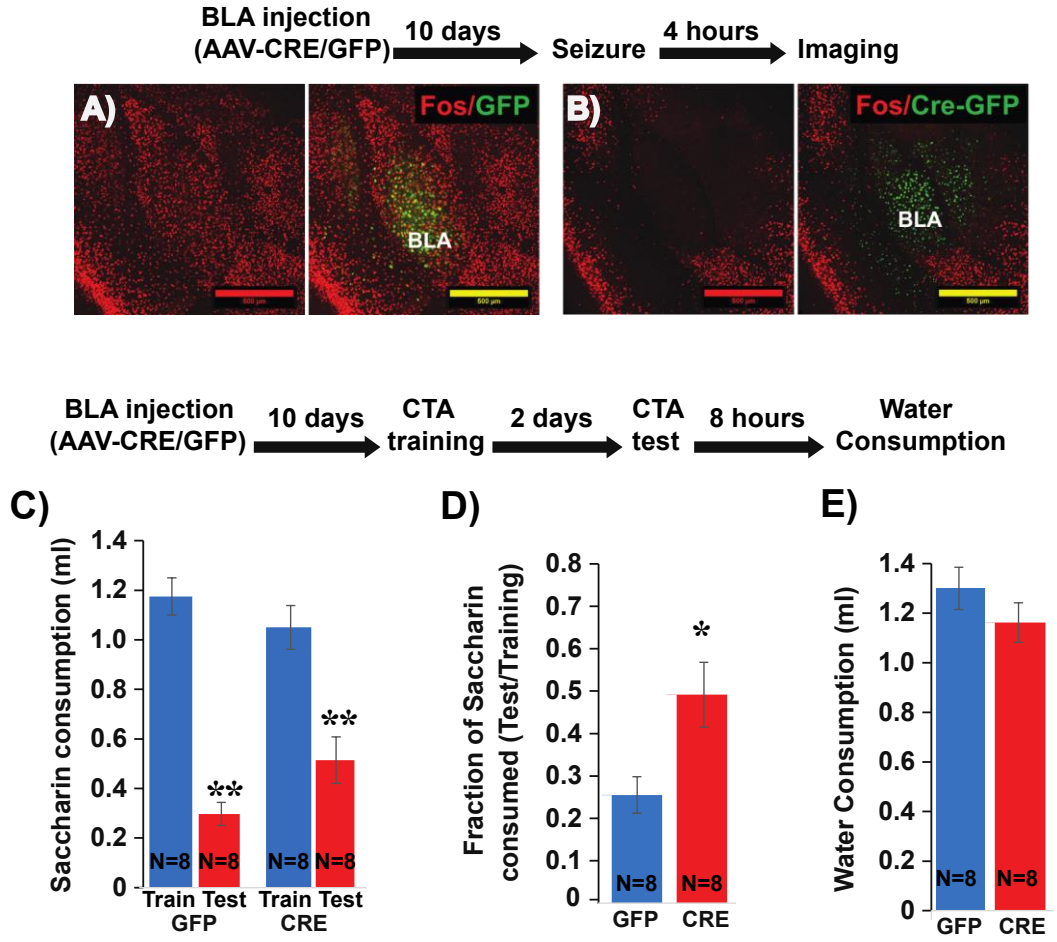

Figure 3. Deletion of Fos from BLApn reduces the strength of learning. (**A,B**) BLA of Fos$^{f/f}$ mice were infected with viruses expressing Cre-GFP **(B)** or GFP alone **(A)**. Fos induction was tested 10 days later, 4 hours after onset of seizures in response to kainic acid (20 mg/kg). Cre injected BLA's had reduced Fos expression confirming penetrance of the knock-out. (**C-E**) Fos deletion from BLApn attenuates CTA learning. Fos f/f mice received Cre and control viruses bilaterally and were trained for CTA 10 days later and then tested after an additional 48 hours. (**C**) Both groups exhibited significant memory reflected by reduced saccharin consumption between training and testing sessions. Two-way ANOVA revealed a significant effect of training ($F(1,28)=63.06$; $p=1.15E-8$), but not of genotype ($F(1,28)=0.261$; $p=0.614$), although there was a significant interaction ($F(1,28)=4.9$; $p=0.03$). Post hoc analysis (Bonferroni) revealed that both GFP (N=8) and Cre (N=8) group reductions following CTA (test vs. train) were significant (GFP: $p=7.17E-8$; Cre: $p=3.47E-4$) but differences between other groups were not. (**D**) Fos deletion from BLApn reduced memory strength measured as the fraction of saccharin consumed (test/training): 25% (GFP) versus 49% (Cre) and this difference in ratios was significant ($t(14)=-2.697$; $p=0.017$). (**E**) Reduced saccharin consumption cannot be attributed to overall inhibition of drinking as the amount of water drunk 8 hours later did not differ ($p=0.26$). *$p<0.05$; **$p<0.01$.

which key exons are flanked by lox-p sites. In both cases, recombination leads to a functionally null allele and analyses were carried out in homozygous ($^{f/f}$) animals. Cre was delivered by injecting AAV2/5-Camk2α::Cre-GFP into the BLA bilaterally. As expected,

this led to GFP expression in excitatory projection neurons, but not in BLA interneurons or adjacent GABAergic neurons in the Central Amygdala (CEA; Figure 3,5). Animals carrying the same genotypes but receiving AAV2/5-Camk2α::GFP served as controls. Injections were performed 10 days prior to analysis to allow time for LOF to occur.

To assess the efficacy of this approach for CTA learning, we first examined the necessity of Fos expression. Fos is known to contribute to multiple forms of learning and plasticity (Zhang et al., 2002; Tonegawa et al., 2015) and has previously been implicated in CTA (Lamprecht and Dudai. 1996; Yasoshima et al., 2006). To first confirm effective Cre-mediated recombination, we tested the ability of viral Cre to prevent widespread Fos expression in the BLA immediately following kainic acid-induced seizures. Fos staining performed four hours after seizures revealed strong induction of Fos protein throughout the BLA of control mice injected with the control virus, and diminished Fos expression in mice injected with Cre (Figure 3A,B). We then tested the effect of Fos deletion on CTA in separate animals. Cre-GFP and GFP control AAV's were injected into the BLA of $Fos^{f/f}$ mice, CTA training occurred 10 days later, and long-term memory was tested after an additional 2 days.
The results show that while both groups could form CTA memory, Cre injected mice showed significantly weaker memory (Figure 3C-E). This confirms our ability to manipulate memory by conditional knockout in BLApn neurons. The results refine those of a prior study using antisense injections and germline knockouts (Yasoshima et al., 2006).

Next, we used the same strategy to test the necessity of Stk11 expression in BLApn for CTA memory. BLA of $Stk11^{f/f}$ mice were injected bilaterally with AAV expressing Cre-GFP, or GFP alone. Ten days later both groups of mice were trained for CTA and tested after an additional two days. The results revealed a near complete loss of learning in the Stk11 KO mice (Figure 4A,B), which exhibited no significant reduction in the amount or ratio of saccharin consumed after training. Control mice exhibited significant reductions consistent with a similar degree of learning to that seen in previous control experiments. The differences in the consumption of saccharin during the test day were not attributable to overall reduced drinking, as both group of animals consumed comparable amounts of water 8 hours later (Figure 4C). Taken together, these results indicate that Stk11 expression in BLApn is essential for CTA memory.

Stk11 deletion prior to CTA training can potentially alter multiple memory stages including memory formation and retrieval (Levitan et al., 2016b). Because CTA memory is long-lasting after even a single training session, it is possible to distinguish an effect of Stk11 deletion on memory formation from an effect on retrieval by performing the deletion immediately after training and before testing. We performed the same knockout and control experiments as those described above, but altered our protocol so that Cre and control viruses were injected 2 days following CTA training. Testing occurred 10 days later, allowing the same period for Cre expression and recombination to occur. Since the memory was being tested after a longer period (twelve days vs. two days), we used a

stronger version of the CTA protocol (I.P injection of 2% LiCl instead of 1%; Figure 4-

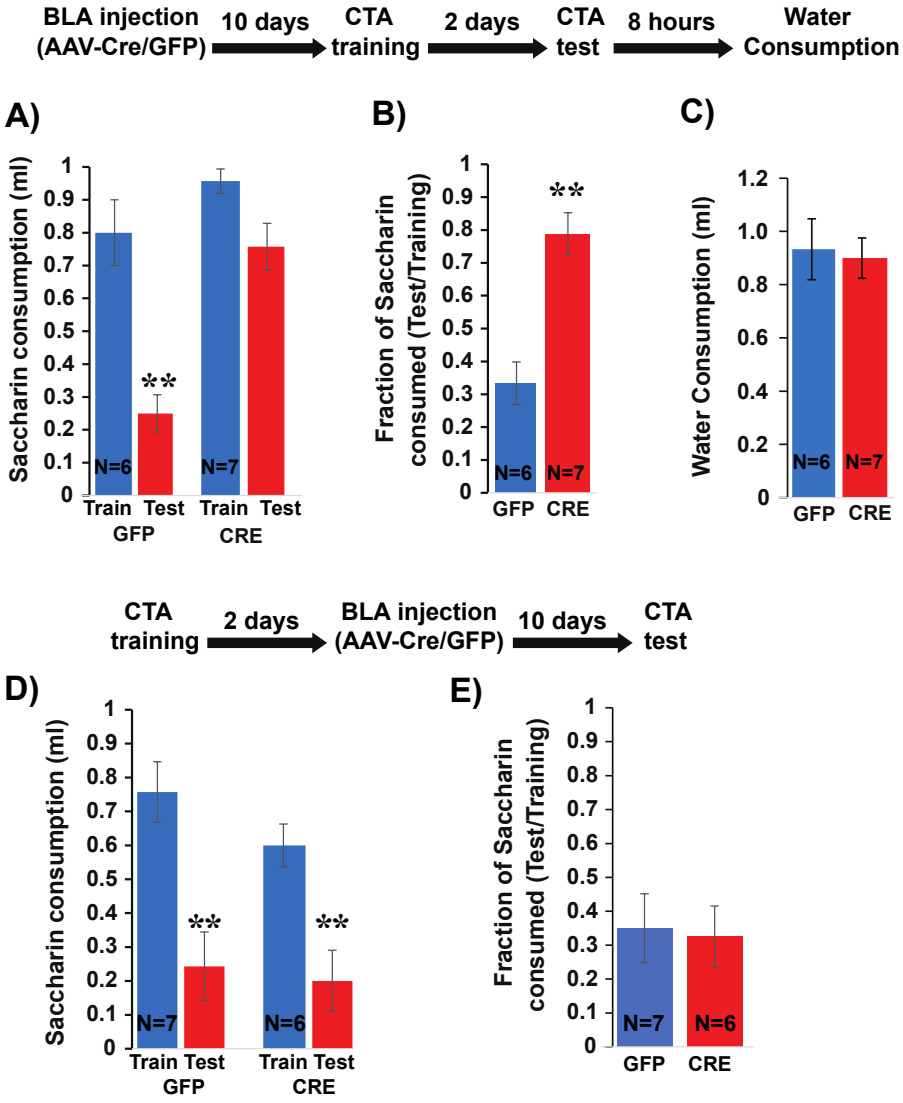

Figure 4. Deletion of Stk11 from BLApn impairs CTA learning. (A) Stk11$^{f/f}$ mice were infected with Cre or control viruses 10 days before CTA training and were tested 48 hours later. Despite significant reduction in saccharin consumption between testing and training sessions in control mice, Stk11 KO animals showed almost no learning. Two-way ANOVA revealed significant group and genotype effects (groups: F(3,22)=19.29; p=0.00002; genotype: F(1,22)=23.43; p=7E-5; as well as a significant interaction: F(1,22)=6.5; p=0.018). Post hoc analysis confirmed that GFP injected mice (N=6) developed strong CTA indicated by the significant reductions (p=0.0001) of saccharin consumption, but Cre injected mice (N=7) failed to significantly reduce their consumption (p=0.259). (**B**) GFP controls consumed only 33% during the test, relative to training, but KO mice consumed 78% and this difference was highly significant (t(11)=-4.91; p=4E-4). (**C**) Reduced saccharin consumption does not reflect overall reduction in drinking measured 8 hours later (t(11)=0.25; p=0.87). **p<0.01. (**D**) Stk11 deletion after long-term memory formation has no effect on CTA retension. Stk11 f/f mice received Cre and control viruses 2 days after CTA training and were tested 10 days later. Two-way ANOVA revealed a significant effect of training

(F(1,22)=21.06; p=8E-6) but no significant effect of genotype (F(1,22)=1.9, p=0.17) or interaction (F(1,22)=0.63, p=0.43). Post hoc analysis confirmed significant reductions in both groups following CTA (GFP: N=7, p=1E-4. Cre: N=6, p=0.006). (**E**) There was no significant difference in CTA intensity as measured by the fraction of saccharin consumed (t=-0.18, p=0.861). **p<0.01.

figure supplement 1).

Both Cre-GFP and GFP injected mice developed CTA (Figure 4D) – there was no significant between-group difference in the intensity of memory, assessed from the ratio of saccharin consumed during the test (Figure 4E). Since the same deletion produces a profound effect when occurring prior to training, this suggests that deletion of Stk11 from BLApn does not affect the retention and retrieval of CTA memory, provided memory was already formed prior to performing the knockout. This argues that Stk11 is required for CTA memory formation.

Stk11 deletion does not impact basal aspects of taste behavior

Since Stk11 deletion must occur prior to CTA training to have an effect on learning, we needed to rule out the possibility that its effect on memory came via disruption of either the responsiveness of BLA neurons to training stimuli, or the output of BLA neurons, which is known to be required for palatability coding within GC.

To assess the responsiveness of BLA neurons to training stimuli, we asked whether training would still activate Fos expression in BLApns after Stk11 deletion. As shown in (Figure 5- figure supplement 1), there is no significant difference between the number of Fos+ neurons following Cre injections and control GFP injections (N=2/group; p<0.05, t-test).

A more rigorous test of BLA function is to determine whether palatability coding in the GC is intact following knockout, since this is known to depend on intact output from the BLA (Piette et al., 2012; Samuelsen et al., 2012; Lin and Reilly. 2012; Lin et al., 2018). If Stk11 deletion disrupts gustatory activation of BLApn or their output to the GC, palatability coding recorded in the GC should be impaired. To test this, Stk11 deletion in BLApn was performed as before and 10 days later multi-channel *in vivo* recordings of GC taste responses were obtained. Recordings were targeted to the ventral part of GC, since BLA projects to these regions (Figure 5A; Haley et al., 2016; Levitan et al., 2019). Palatability coding was assessed with a battery of four tastes with hedonic values ranging from palatable (sucrose and sodium-chloride) to aversive (citric-acid and quinine; for details see Levitan et al., 2019).

Figure 5 shows the results of GC taste responses following Stk11 deletions in BLA. Figure 5B illustrates the peri-stimulus histogram of a representative GC neuron responding to the taste battery. As observed previously in rats and mice (Katz et al., 2001; Sadacca et al., 2013; Levitan et al., 2019), different aspects of taste processing are encoded in firing rates sequentially. In the first five hundred milliseconds or so post-taste delivery, neurons show different firing rates to different tastes (i.e., reflecting taste identity coding), while

later in the responses, differential response rates reflect the hedonic values of tastes (i.e., taste palatability coding). These properties were maintained in the mice studied here: as indicated by the dashed line, the magnitude of the correlation between the neuron's stimulus evoked firing rates and the behaviorally-determined palatability ranking rose significantly only after the first half a second following taste delivery. The averaged correlation magnitudes across neurons from Cre and GFP injected mice are shown in Figure 5C. Inspection of the figure suggests that BLA Stk11 deletion had little effects on GC taste palatability coding; the correlations in both GFP- and Cre-injected groups rise around half a second and peaks at about one second after taste delivery. An ANOVA found no significant group differences across each time bin, suggesting that Stk11 deletion in BLA has little detectable influence on GC taste processing.

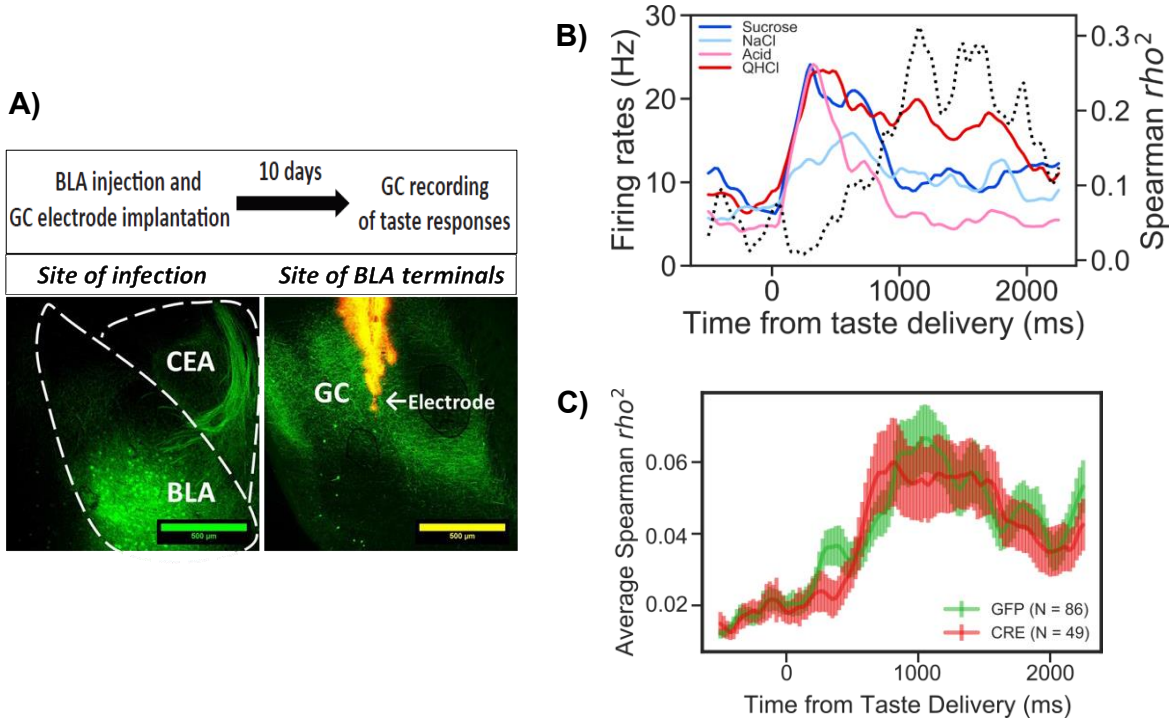

Figure 5. Stk11 deletion in BLApn does not affect taste palatability coding in the GC. (**A**) The BLA of Stk11$^{f/f}$ mice was infected bilaterally with Cre or control viruses. The ventral GC, where BLA projections terminate (Haley et al., 2016) was implanted with a multi-electrode array 10 days later to record GC taste responses to a battery of four tastes differing in their hedonic value, the palatable sucrose and sodium-chloride and the aversive critic acid and quinine (Levitan et al., 2019). Images show BLA injection site (left), and labeled BLA terminals in the ventral GC co-localized with the site of dye-labeled electrodes (right). (**B**) PSTHs (colored lines) from a representative GC neuron in a GFP-injected control mouse that responded significantly to all tastes. Dashed line represents the magnitude of correlation between firing rates and behaviorally measured palatability. (**C**) Correlation coefficients averaged across all recorded units in GFP(control) and Cre- injected mice. As revealed in a 2-way ANOVA, palatability correlations in both groups rise steeply between 800-1000 ms with no significant difference between genotypes ($F(1,133)=0.13$, $p = 0.72$) or interaction ($p =0.99$).

Taken together, our molecular and electrophysiological analyses suggest that the memory deficit observed after Stk11 deletion is unlikely to be due to a deficit in basic taste processing. Rather, Stk11 deletion likely impairs memory by affecting the process of memory formation.

Stk11 or Fos deletion and CTA produce opposing effects on BLA intrinsic excitability

What cellular mechanisms mediate the effects of Fos and Stk11 on memory formation? Obvious candidates abound: for instance, long-term memory is known to be accompanied by changes in both the intrinsic excitability of neurons (Zhang and Linden, 2003; Mozzachiodi and Byrne, 2010) and in the strength of their synaptic connections. Recent studies have shown that the intrinsic excitability of BLApn can be modulated bi-directionally during reinforcement learning, with positive reinforcement leading to increased and negative reinforcement to decreased intrinsic excitability (Motanis et al., 2014).

To determine whether Stk11 might influence memory formation by altering intrinsic excitability, we compared the excitability of BLApn recorded in ex-vivo slices from mutant animals receiving Cre-GFP (Figure 6). The results reveal a marked increase in the intrinsic excitability of BLApn following deletion of Stk11, relative to GFP-only controls. Cre infected neurons had higher firing rates than GFP

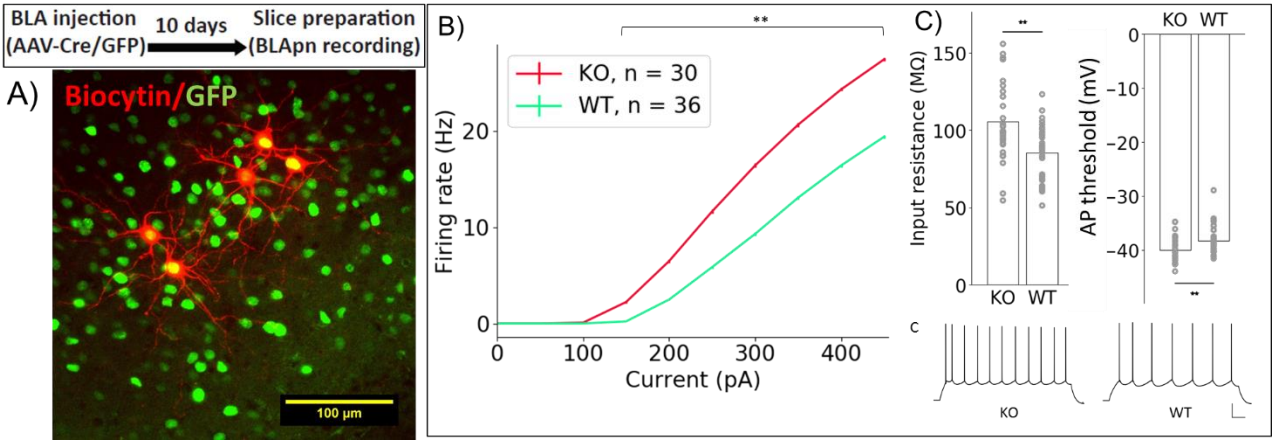

Figure 6. Stk11 deletion in BLApn increases intrinsic excitability. (**A**) Whole-cell recordings obtained from BLApn in *ex vivo* slices of Stk11$^{f/f}$ mice 10 days after injection of Cre or control virus. Stk11 neurons were targeted based on GFP expression and validated post hoc based on Biocytin fills. (**B**) Firing rates plotted against input current (F-I). Error bars (SEM) are too small to be seen for some points. Less current is needed to evoke firing in Stk11-KO neurons compared to Stk11-WT neurons (interpolated rheobase, F(1,64) = 10.63, p = 1.8e-3). The F-I slope is larger for Stk11 knockout neurons (F(1,64) = 23.47, p = 8.4e-6). (C**)** Stk11-KO neurons have increased input resistance (F = 14.41, p = 3.3e-4) and decreased threshold for generating action potential (F = 7.68, p = 7.3e-3). Traces are sample responses to 300 pA current steps. Scale bar: 100 ms, 20 mV.

neurons for any given amount of current input resulting in a steeper slope of the firing rate vs. current (F-I) curve. Threshold firing was initiated at a lower level of current injection (i.e. the rheobase was lower; Figure 6C). This reflected a higher resting input resistance and a slightly lower voltage threshold. Some other electrophysiological properties also differed (see Table 4) including sag ratios, action potential amplitudes, and the medium and slow afterhyperpolarizations, while others, such as the degree of firing rate accommodation, spike widths and resting membrane potentials did not. Thus, Stk11 deletion from BLApn neurons increases overall intrinsic excitability, most likely by affecting multiple biophysical properties of these neurons.

Since Stk11 and Fos deletion both impair CTA learning, we wondered whether Fos deletion also increases the intrinsic excitability of BLApn. Analysis of Fos KO neurons revealed a similar increase in firing relative to control neurons (N for: WT=14, KO=22; Figure 7A-B). Two-way ANOVA indicated a significant effect of genotype (in addition to the expected effect of current level). Significant differences in input resistance and action potential threshold were also detected.

Finally, we asked whether we could detect an effect of learning itself on neuronal excitability in the BLA. A difficulty with this experiment is that learning may have different effects on different populations of BLApn as evidenced by the fact that some neurons increase Fos expression following training, while others do not (Figure 2-figure supplement 2). In order to separately examine these two populations following training, we made use of the reporter system developed by Reijmers and colleagues, in which elements of the Fos promoter are used to drive the tet transactivator (tTA) which can then prolong and amplify expression of a reporter marking Fos-activated cells, when Doxycycline (Dox) is absent (Reijmers et al., 2007). In this case, we provided the tet-dependent reporter via an AAV (TRE::mCherry) injected into the BLA ten days prior to training. Animals were fed Dox until 24 hours prior to training to limit background activation (Figure 7C). Control experiments showed that CTA training resulted in a greater number of neurons expressing Fos 24 hours after training, compared to home cage controls (Figure 7D). Twenty-four hours following CTA training or taste-only control experiments, recordings were obtained from BLApn in acute slices. Two-way ANOVA revealed that BLApn in the CTA animals have lower input resistance than those in control animals and that Fos-activated neurons have lower input resistance than unlabeled neurons (Figure 7E). Notably, this change is in the opposite direction from that produced by deletions of Stk11 and Fos, two manipulations that impair learning. This suggests that these mutations may interfere with learning by impairing changes in intrinsic excitability that are required for learning to occur.

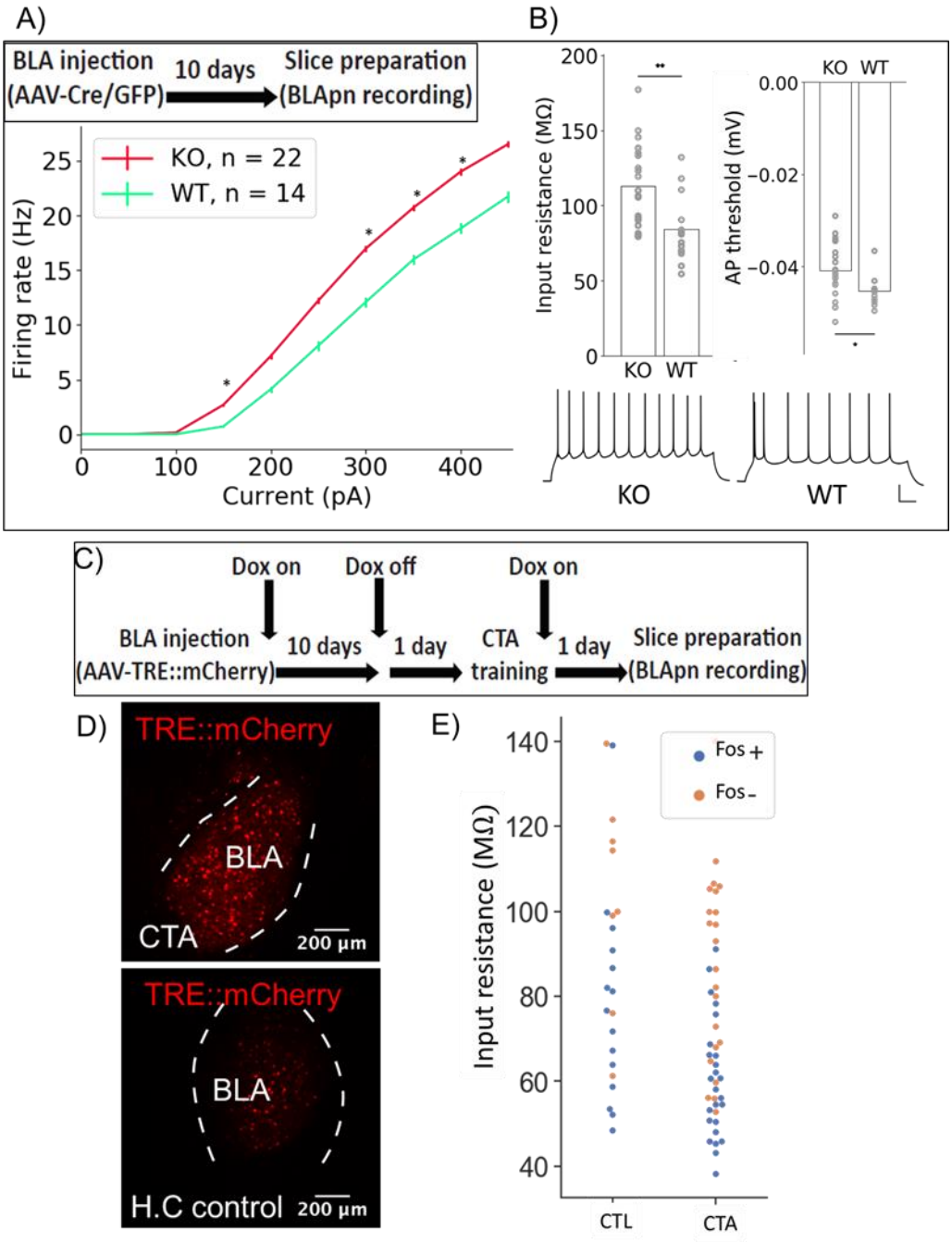

Figure 7. **Fos deletion and CTA have opposing effects on resting input resistance**. (**A,B**) Whole-cell patch-clamp recordings obtained from BLApn in *ex vivo* slices of $Fos^{f/f}$ mice 10 days after injection of Cre or control virus. Fos-KO neurons exhibit increased firing in response to current injection compared to Fos-WT neurons. **(A)** Average frequency-current (FI) curves. Two-way mixed ANOVA revealed a significant difference in firing $F(1,34) = 4.213$, $p = 0.045$. (**B**) Significant differences in input resistance ($F(1) = 10.62$, $p = 2.5e\text{-}3$) and threshold for generating action potential ($F(1) = 6.82$, $p = 0.013$) between Fos-KO and Fos WT neurons were also detected. Sample responses to 250 pA current steps. Scale bar: 100 ms, 20 mV. (**C**) Tet-dependent labeling of Fos expressing neurons (Reijmers et al., 2007) during CTA training.

Fos::tTa mice were injected with AAV-TRE::mCherry and received food with 40 ppm Doxycycline (Dox) to suppress reporter expression. One day prior to CTA training, Dox was removed. Acute slices were prepared 24 hours following CTA (Saccharin+lithium) or control (Saccharin+saline) training. (**D**) Fos expressing neurons labeled through Tet-off system with mCherry fluorescent reporters in the BLA. (**E**) Input resistances of $Fos^{+/-}$ neurons in the BLA, following CTA training and taste-only control experiments. Two-way ANOVA reveals that neurons from CTA animals have lower input resistance than those from control animals ($F(1,65) = 10.26$, $p = 2.1e\text{-}3$) and that Fos^{+} neurons have lower input resistance than Fos^{-} neurons ($F(1,65) = 23.64$, $p = 7.5e\text{-}6$). Post-hoc tests show that among Fos^{+} neurons, neurons in CTA animals have lower input resistance ($p = 0.015$), while among Fos^{-} neurons, there was no significant difference between CTA and control animals ($p = 0.1$). Differences between Fos^{+} and Fos^{-} neurons did not reach post-hoc significance in either the CTA ($p = 0.25$) or control animals ($p = 0.12$) considered alone.

Discussion

This study is the first to identify a role for Stk11, a master kinase at the top of the AMP-related kinase pathway, in long-term memory. Using CTA as a behavioral paradigm, we first established a causal requirement for transcription in BLApn during establishment of long-term memory, and went on to show that changes in Stk11 transcription and translation accompany CTA learning. Cell-type specific conditional knock-out of Stk11 in BLApn revealed it to be necessary for CTA memory formation but not for retrieval, once memories were established. Slice recordings revealed that Stk11 modulated the intrinsic excitability of these neurons and further investigations suggested the general importance of excitability changes for memory—deletion of the immediate early gene Fos in BLApn altered excitability similarly to Stk11 deletion, and conversely activation of Fos during learning reduced excitability.

BLA projection neurons undergo transcription important for CTA learning

It is well established that BLA neurons play a necessary role in CTA learning. Multiple studies confirm that activity in the BLA is required for memory formation and retrieval (Yasoshima et al., 2000; Ferreira et al., 2005; Garcia-de la Torre et al., 2014; Molero-Chamizo, et al., 2017). CTA also requires protein synthesis in the BLA (Josselyn et al., 2004), but whether new transcription is also required, and if so, the identities of the required transcripts and the cellular processes they promote were not previously known.

Here we show that BLA projection neurons (BLApn) undergo transcriptional changes important for CTA memory. Inhibiting transcription during CTA training impairs memory tested 48 hours later. Using cell-type specific RNA sequencing, we go beyond this simple insight to identify the transcripts that are altered in expression in BLApn four hours after pairing of the conditioned and unconditioned stimuli. For comparison, we also examined changes in transcript levels in pyramidal neurons and parvalbumin-positive interneurons in gustatory cortex. These profiling experiments provide a resource for future investigations of other molecules potentially involved in CTA in BLA and GC.

Perhaps the strongest case for new transcription in BLApn involved in learning can be made for the immediate early gene Fos. It is well known that Fos transcription and translation are activated in the forebrain by a variety of memory paradigms (Mayford and Reijmers. 2015), and more specifically by CTA in BLApn (Uematsu et al., 2015). The YFP-H neurons studied here include the majority of BLApn in the anterior portion of the nucleus (Feng et al., 2000; Sugino et al., 2006; Jasnow et al., 2013; McCullough et al., 2016) and the fact that many of these neurons express Fos protein (Figure 2-figure supplement 1) and project to GC (Figure 5A and Haley et al., 2016) supports the suggestion that they are among the population of BLApn transcriptionally activated by training and participating in the BLA-GC circuit implicated in learning by prior studies (Grossman et al., 2008). Since Fos transcript and protein are short-lived (Spiegel et al., 2014; Chowdhury and Caroni. 2018) the most parsimonious explanation is that training induces new transcription and translation, and that it is these effects that are disrupted by the Fos KO in BLApn (Figure 3). Nevertheless, even for Fos, we cannot rule out the possibility that effects of the knockout preceding training, such as altered excitability, are what are necessary for learning, rather than new transcription and translation immediately following learning. Resolution of this issue will require new technologies like protein knockout (Clift et al., 2017) with temporal resolutions measured in minutes rather than days.

The results of selectively knocking Fos out in BLApn clarify the results of earlier studies in which Fos was manipulated with infusion of antisense oligonucleotides (Lamprecht et al., 1996; Yasoshima et al., 2006) or via global knockout (which had no effect on CTA; Yasoshima et al., 2006). Loss of memory has previously been attributed to inhibition of Fos in central amygdala (Lamprecht et al., 1996), or in the amygdala as a whole along with the GC (Yasoshima et al., 2006). Our demonstration that knockout restricted to BLApn is sufficient to impair memory does not contradict these earlier studies, but suggests that these projection neurons may be a nexus or bottleneck vital for learning in the circuit.

There is still much to be learned about the specific involvement of new transcription of Stk11 in CTA. This transcript is presumably less transient than that of immediate early genes, and may be part of a process with complex dynamics. This issue is brought into focus by the fact that, across the time points measured, the transcript in profiled cells was decreased, while in anatomically sub-dissected portions of BLA, Stk11 protein was increased. Improved temporal and spatial mapping of transcript and protein levels will clarify the nature of the process. Regardless, however, loss of function confirms the necessity of Stk11 expression within BLApn for CTA learning.

Necessity of Stk11 implicates the AMP-related kinase pathway in learning

Prior studies of CTA and other forms of aversive learning in the BLA have implicated a number of kinases: including those in the cAMP-dependent protein kinase, protein kinase C, extracellular signal-regulated, and mitogen-activated protein kinase pathways (Johansen et al., 2011; Adaikkan and Rosenblum, 2012). Each of these also have well

established roles in other forms of forebrain learning and plasticity (Alberini, 2009). Here we reveal the likely involvement of another kinase cascade, well studied in the contexts of cell growth, metabolism, cancer and polarity (Shackelford and Shaw. 2009) but hitherto unstudied in the context of learning and memory. That this pathway should have a role in learning is perhaps not shocking given the ubiquity of its previously demonstrated roles in 1) axonal development (Barnes et al., 2007; Shelly et al., 2007); 2) synaptic remodeling during aging (Samuel et al., 2014); 3) regulation of presynaptic neurotransmission (Kwon et al. 2016); and perhaps most tellingly 4) regulation of glucose metabolism, feeding and obesity through actions in multiple tissues including hypothalamus (Xi et al., 2018; Fei-Wang et al., 2012; Claret et al., 2011). Given the involvement of hypothalamus in coding of taste palatability, and the connectivity between hypothalamus and gustatory cortex (Li et al., 2013), it is tempting to speculate that the role of Stk11 signaling pathways in feeding may be functionally related to its role in gustatory learning. Further studies will be needed to distinguish whether the involvement of Stk11 in memory is specific to forms of learning regulating consumption, and whether its role in CTA learning is confined to the basolateral amygdala.

Stk11 is a master kinase that regulates the activity of 13 downstream AMP-related kinases with diverse roles (Lizcano et al., 2004). Prkaa1/2 (also known as AMPK) is crucial for metabolic regulation during altered levels of nutrients and intracellular energy. BRSK and MARK regulate cell polarity during development (Barnes et al., 2007; Shackelford and Shaw. 2009). We found that, while Prkaa1/2 and several other downstream kinases have low levels of expression in BLApn, others, including Mark2 and 3, are expressed at higher levels (Figure 2-figure supplement 3). Furthermore, changes in MARK2 and Stk11 expression were correlated during CTA learning. During axonal development, BDNF and cAMP signaling require the Stk11/MARK cascade (Barnes et al., 2007; Shelly et al., 2007). BDNF and cAMP are also implicated in CTA (Ma et al., 2011; Koh et al., 2002; Koh et al., 2003), raising the possibility that these signaling pathways also intersect during learning.

Deletion of Stk11 prior to training profoundly impaired memory, but deletion two days after training—when memory formation and consolidation have already occurred (Alberini, 2009; Gal-Ben-Ari et al., 2012; Bambha-Mukku et al., 2014; Levitan et al., 2016) —did not. This suggests that Stk11 expression in BLApn promotes memory formation, rather than memory maintenance or retrieval. It is clear that Stk11 deletion left much of the machinery of taste processing and learning intact, however. Activation of Fos by training in the BLA was not impaired after Stk11 deletion, implying that at least the initial stages of transcriptional activation associated with learning are intact. Also left intact was the ability of the BLA to convey palatability information to the GC. Prior studies have shown that silencing of BLA neurons, or of their axons within the GC, impair palatability coding during the late phase of GC gustatory responses. We found that these responses were still present in GC following knockout, implying that this critical function of the BLA for CTA learning remained intact.

Intrinsic excitability of BLApn as a candidate mechanism for Fos and Stk11's effects on CTA memory.

Learning paradigms that support synaptic plasticity also frequently induce changes in neuronal excitability, and such plasticity of intrinsic excitability has long been known to accompany classical conditioning in the neocortex, olfactory cortex, hippocampus, amygdala and cerebellum (for reviews see Zhang and Linden, 2003; Frick and Johnston, 2005; Mozzachiodi and Byrne, 2010; Titley et al. 2017; Debanne et al. 2019).

In our hands, two genetic manipulations of BLApn that impair learning also increase the intrinsic excitability of BLApn, whereas BLAp involved in normal conditioning appear to experience the opposite change. This suggests an important role in learning for excitability changes, and begs the question of mechanism. Although there are likely multiple such mechanisms, the increase in excitability partly reflects an increase in the resting input resistance and a corresponding decrease in the threshold current needed to evoke firing. It is worth noting that most prior studies of intrinsic plasticity have reported increases in excitability with learning (Zhang and Linden, 2003; Mozzachiodi and Byrne, 2010; Pignatelli et al., 2019). Our results are not without precedent, however; and are similar in polarity to those found in BLApn following olfactory fear conditioning, another form of negative reinforcement learning (Motanis et al., 2014). Decreased excitability of Fos-activated neurons was also found using an earlier reporter of Fos promoter activation (Yassin et al., 2010).

In conclusion, we have demonstrated dual roles for the kinase Stk11 in BLApn. Conditional deletion increases their neuronal excitability and at the same time blocks acquisition of CTA memory without altering baseline contributions to taste coding or the ability to undergo the initial stages of transcriptional activation during training. Further work will be needed, first, to map out the intervening steps by which Stk11 affects downstream signaling partners leading to increased excitability and reduced learning, second, to better understand how these pathways intersect with transcriptional activation of immediate early genes, and third, to determine whether, and if so how, cellular changes in excitability and behavioral changes in learning are causally related.

Material and Methods

Subjects

Male and Female mice were used for behavior at age 60-80 days, or for electrophysiology at 25-35 days. Strains: wild-type; WT (C57BL/6J), YFP-H (B6.Cg-Tg(Thy1-YFP)HJrs/J), $Stk11^{f/f}$ (B6(Cg)-Stk11tm1.1Sjm/J, Lkb1fl), $Fos^{f/f}$ (B6;129-Fostm1Mxu/Mmjax), Fos-tTA (B6.Cg-Tg(Fos-tTA,Fos-EGFP*)1Mmay/J) all purchased from Jackson Laboratories (Bar Harbor, ME, USA). Mice were placed on a 12-hour light-dark cycle, and given *ad libitum* access to food and water except during training, at which time water access was

restricted, while food remained available *ad libitum* (note that animals reliably consume less food when thirsty). All procedures were approved by the Brandeis University Institutional Animal Care and Use Committee (IACUC) in accordance with NIH guidelines.

Surgery

BLA cannulation for RNA synthesis inhibition experiments: WT Mice were anesthetized via ip injections of 100µg ketamine, 12.5 µg xylazine, 2.5 µg acepromazine per gram (KXA). Guide cannulae (23-gauge, 10 mm length) were implanted above the BLA (mm from bregma, AP= -1.4, DV= 4.2, ML= ±3.4) and stabilized using Vetbond and dental acrylic. Stainless steel stylets (30-gage, 10mm) were inserted into the guide cannula to ensure patency. Mice received postsurgical metacam (5 µg/g), penicillin (1500 Units/g) and saline (5 % body-weight) per day for three days and recovered a total of 7 days prior to training. Twenty minutes prior to CTA training, mice were infused with either 50 ng of actinomycin-D or vehicle control (PBS) bilaterally (in 1 µl over 2 minutes) via infusion cannulae extending 0.5 mm below the guide cannulae to reach the BLA. Each cannula was connected to a 10µl Hamilton syringe on a syringe pump (Harvard Apparatus, Massachusetts, MA, USA).

BLA viral infection: $Stk11^{f/f}$, $Fos^{f/f}$ and Fos-tTA mice were anesthetized with KXA. The skull was exposed, cleaned, and bilateral craniotomies were made at stereotactic coordinates (AP= -1.4, ML= ±3.4). BLA were injected bilaterally with AAV2/5-Camk2α::Cre-GFP or AAV2/5-Camk2α::GFP (UNC, vector core) for $Stk11^{f/f}$ and $Fos^{f/f}$ mice and AAV2/5-TRE::mCherry for Fos-tTa mice, 10 days prior to CTA training using sterile glass micropipettes (10-20 µm diameter) attached to a partially automated microinjection device (Nanoject III Microinjector, Drummond Scientific). The micropipettes were lowered to 4.3 mm and 4.6 mm from the dura to reach the BLA. At each depth, virus (200 nl) was delivered via 10 pulses of 20 delivered every 10 sec, with 10 min between each injection. Postsurgical treatment and recovery were as above.

Conditioned Taste Aversion (CTA): Mice were housed individually with free access to food and maintained on a 23.0 h water deprivation schedule for the duration of training and experimentation. Three days prior to CTA training, water bottles were removed from the cages and water was given twice a day (10 am and 6 pm) for a duration of 30 min. On the day of CTA mice were given 30 min to consume 0.5 % saccharin, which was followed by intraperitoneal (I.P) injection of lithium-chloride (0.15M, 2% of body weight, unless indicated differently) 30 min later. Taste control groups received I.P injection of saline (0.9 % sodium chloride) instead of lithium and lithium control group received lithium injection alone 24 hours following Saccharin consumption. CTA testing: Mice were kept on watering schedule twice a day and 48 hours after CTA training mice received CTA testing which consisted of 30 min consumption of 0.5 % saccharin. 8 hours following testing mice were given 30 min water consumption.

Seizure induction: $Fos^{f/f}$ mice were housed individually with free access to water and food and received BLA viral infection with Cre and control viruses as described above.

After 10 days, mice were injected I.P. with 20 mg/kg kainic acid in PBS. Four hours after injection, mice were perfused for Fos immunohistochemistry.

Immunohistochemistry: Mice were deeply anesthetized with an overdose of KXA and perfused transcardially with phosphate buffered solution (PBS) followed by 4% paraformaldehyde (PFA). Brains were post-fixed in PFA for 1-2 day, and coronal brain slices (60 µm) containing the BLA (-1mm to -2.5 mm anterior-poterior axis) were sectioned on a vibratome. Slices were rinsed with PBS and incubated in a blocking solution (PBS/.3%TritionX-100/5% Bovine serum albumin) for 12-24 hours at 4ºC. Blocking solution was removed and replaced with the primary antibody solution which consists of 1:100 c-Fos polyclonal rabbit IgG (SC-52G; Santa Cruz Biotechnology) for 24 hours at 4ºC. After incubation, slices were rinsed using a PBS/.3% Triton X-100 solution followed by the secondary antibody incubation of 1:500 c-Fos Alexa Flour 546 Goat-Anti-Rabbit IgG (H+L) (Life Technologies) and 5% natural goat serum for 12-24 hours at 4ºC. Sections were then rinsed 5-6 times over 90 mins (1XPBS/.3% Triton X-100), counterstained with DAPI, mounted with antifade mounting medium (Vectashield), and viewed by confocal fluorescence microscopy (Leica Sp5 Spectral confocal microscope/Resonant Scanner). Imaging and quantification were performed blind to experimental group.

Fos quantification and analysis: To minimize systematic bias, Fos counts were performed blind and semi-automatically, using FiJi (University of Wisconsin-Madison; Schindelin et al. 2012). Eight-bit images were binarized and particles smaller than 10 μm^2 were rejected. Each cell count was from a separate animal and was the average of counts from six sections through the anterior, middle and posterior regions of the BLA of both hemispheres.

RNA sequencing experiment: RNA sequencing was performed on YFP^+ BLApn harvested from male YFP-H mouse line (Feng et al., 2000; Sugino et al., 2006; Jasnow et al., 2013; McCullough et al., 2016) which expresses YFP under the Thy1 promoter in the majority of excitatory projection neurons located in the anterior part of the nucleus. The mice underwent CTA training or taste-only controls (n=4/group) and 4 hours following training were subjected to manual cell-sorting, performed as previously described (Sugino et al, 2006; Hempel et al; 2007; Shima et al., 2016) by dissociating 150-200 fluorescently labeled neurons in 300µm thick brain slices and manually purifying them through multiple transfer dishes with the aid of a pipette viewed under a fluorescence dissection microscope. Total RNA was extracted from sorted cells using Pico-pure RNA isolation kit (Thermo fisher). Amplified cDNA libraries are prepared from isolated, fragmented RNA using the NuGen Ovation RNAseq V.2 kit (NuGEN, San Carlos, CA) and followed by purification using the Beckman coulter Genomic's Agencourt RNA Clean XP kit and Zymo DNA Clean & Concentrator. Sequencing adaptors are ligated per Illumina protocols and 50 bp single-ended reads are obtained from Illumina Hi-Seq machine. Libraries sequenced usually results in 25-30 million unique reads using 8-fold multiplexing.

Analysis: Reads are trimmed and then aligned to the mouse genome using TopHat (Trapnell et al. 2012). Sam files are converted to binary format using Samtools and visualized at the sequence level using IGV. Script written in python and R statistical package are used to convert unique reads to gene expression values and to filter genes by relative expression and statistical significance.

qPCR validation: The brains of a separate group of YFP-H mice receiving CTA (taste+lithium, N=4) or taste control (taste+saline, N=4) were harvested 4 hours following the end of the training and subjected to fax sorting. RNA was extracted using pico-pure kit and reverse transcribed to cDNA using iScript cDNA synthesis kit. qPCR was performed on Rotor-Gene qPCR machine using PCR master mix and transcript-specific sets of primers for Fos, Stk11 as target genes and Snap47 as loading control.

Acute slice electrophysiology: Ten days after virus injection, acute brain slices were prepared from P28-35 mice. Animals were deeply anesthetized with KXA and transcardially perfused with ice-cold oxygenated cutting solution containing (in mM): 10 N-methyl-D-glucamine (NMDG), 3 KCl, 1 NaH2PO4, 25 NaHCO3, 20 HEPES, 2 Thiourea, 3 Sodium Pyruvate, 12 N-acetyl-L-cysteine, 6 MgCl2, 0.5 CaCl2, 5 Sodium Ascorbate, 10 Glucose (pH: 7.25 – 7.4, adjusted using HCl). 300 µm coronal slices containing the BLA were cut on a vibratome (Leica), and then recovered for 15 min at 33 °C and for 15 min at room temperature in oxygenated recovery solution containing (in mM): 74 NaCl, 3 KCl, 1 NaH2PO4, 25 NaHCO3, 6 MgCl2, 0.5 CaCl2, 5 Sodium Ascorbate, 75 Sucrose, 10 Glucose, followed by at least another 1 hour at room temperature in oxygenated ACSF containing (in mM): 126 NaCl, 3 KCl, 1 NaH2PO4, 25 NaHCO3, 2 MgCl2, 2 CaCl2, 10 Glucose. During recordings, slices were perfused with oxygenated 34-35 °C ASCF. Target neurons in BLA were identified based on the presence of viral GFP reporter. ACSF included 35 µM d,l-2-amino-5-phosphonovaleric acid (APV) and 20 µM 6,7-dinitroquinoxaline-2,3-dione (DNQX) to block ionotropic glutamate receptors, and 50 µM picrotoxin to block ionotropic GABA receptors. Whole-cell recording pipettes (6 – 8 MΩ) were filled with internal solution containing (in mM): 100 K-gluconate, 20 KCl, 10 HEPES, 4 Mg-ATP, 0.3 Na-GTP, 10 Na-phosphocreatine, and 0.1% biocytin. Recordings were amplified (Multiclamp 700B, Molecular Devices) and digitized at 10 kHz using a National Instruments Board under control of IGOR Pro (WaveMetrics). Resting membrane potentials were adjusted to -70 mV and steady state series resistance was compensated. Series resistance and input resistance were calculated using -5 mV (voltage clamp) or 25 pA (current clamp) seal tests before each trial of recording. Measurements of input resistance in Fos reporter labeled neurons (Figure 7) were measured in voltage clamp, all other recordings were performed in current clamp. The calculated liquid junction potential (-10 mV) was compensated post hoc. Neurons with high series resistance (> 30 MΩ current clamp) or membrane potentials that changed by > 10 mV were excluded. Hyperpolarization activated sag was measured from responses to -100 pA current steps. Action potential (AP) threshold, amplitude, afterhyperpolarization (AHP) and full width at half-height were averaged from the 5th-10th APs in trials with 10 to 20 Hz firing rates. AP threshold is the membrane potential at which

739 the slope first exceeds 10 V/s, and AP amplitude was measured relative to threshold. Sag
740 ratio is defined as the fraction by which the membrane potential depolarized at steady-
741 state from its maximum hyperpolarization during a -100 pA current step. Medium AHP
742 was measured as the peak hyperpolarization after the APs mentioned above relative to
743 threshold. The slow AHP was measured from the peak hyperpolarization following
744 positive current steps generating 10-20 Hz firing.

745 ***In-vivo recording of GC taste responses***

746 ***Surgery:*** Stk11$^{f/f}$ mice were anesthetized and prepared for stereotaxic surgery and viral
747 infection as above. Each mouse was also implanted bilaterally with multi-channel
748 electrode bundles (16 formvar-coated, 25-µm diameter nichrome wires) in GC (Distance
749 from Bregma: AP=+1.2mm; ML=±3 mm; DV of -2.25 mm from the *pia mater*) and a single
750 intraoral cannula (IOC; flexible plastic tubing) was inserted into the cheek to allow
751 controlled delivery of taste stimuli. 24 hours before recording sessions began electrode
752 bundles were then further lowered by 0.75-1.00 mm to reach ventral GC (see Figure 5A).

753 ***IOC Fluid delivery protocol:*** Experiments began with three days of habituation to the
754 recording setup and to receiving liquid through the IOC. Sixty 15-µl aliquots (hereafter,
755 "trials") of water were delivered across 30 min. To ensure adequate hydration, mice were
756 given two 30 min period of access to additional water.

757 On the following day, recording commenced and water trials were replaced with 4
758 different taste stimuli: sweet (0.2 M sucrose), salty (0.1 M sodium chloride), sour (0.02 M
759 citric acid), and bitter (0.001 M quinine). A total of 15 trials were delivered for each taste
760 in random order. These tastes and concentrations were chosen because they provided a
761 broad range of hedonic values for palatability assessment. Fluid delivery through a
762 nitrogen-pressurized system of polyethylene tubes was controlled by solenoid valves via
763 a Raspberry Pi computer (construction details and code available on request from
764 [https://github.com/narendramukherjee/blech_clust].

765 ***Taste palatability coding:*** To determine whether a neuron displays palatability activity,
766 we performed a moving window analysis (window size: 250 ms; step size: 25 ms) to trace
767 the dynamics of taste processing in GC. For each time window, we calculated a
768 Spearman product-moment correlation between the ranked firing rates to each taste and
769 the palatability rankings obtained previously in separate experiments (Levitan et al.,
770 2019).

771 ***Statistical analysis***: The results are expressed as means ± s.e.m unless otherwise
772 stated. All effects were evaluated using either paired t-test or one- or two-way ANOVA
773 test with post hoc t-tests corrected (Bonferroni) for all possible pair-wise comparisons.

774

References

Adaikkan C, Rosenblum K (2012) The role of protein phosphorylation in the gustatory cortex and amygdala during taste learning. Exp Neurobiol 21:37-51.

Alberini CM (2009) Transcription factors in long-term memory and synaptic plasticity. Physiol Rev 89:121-145.

Allen Institute for Brain Science. Allen Mouse Brain Atlas. Available from: mouse.brain-map.org (2008).

Bailey CH, Kandel ER, Harris KM (2015) Structural Components of Synaptic Plasticity and Memory Consolidation. Cold Spring Harb Perspect Biol 7:a021758.

Bambah-Mukku D, Travaglia A, Chen DY, Pollonini G, Alberini CM (2014) A positive autoregulatory BDNF feedback loop via C/EBPbeta mediates hippocampal memory consolidation. J Neurosci 34:12547-12559.

Barnes AP, Lilley BN, Pan YA, Plummer LJ, Powell AW, Raines AN, Sanes JR, Polleux F (2007) LKB1 and SAD kinases define a pathway required for the polarization of cortical neurons. Cell 129:549-563.

Barot SK, Kyono Y, Clark EW, Bernstein IL (2008) Visualizing stimulus convergence in amygdala neurons during associative learning. Proc Natl Acad Sci U S A 105:20959-20963.

Bures J, Bermúdez-Rattoni F, Yamamoto T. 1998. Conditioned taste aversion: Memory of a special kind. Oxford University Press, New York, NY, US.

Carleton A, Accolla R, Simon SA (2010) Coding in the mammalian gustatory system. Trends Neurosci 33:326-334.

Chowdhury A, Caroni P (2018) Time units for learning involving maintenance of system-wide cFos expression in neuronal assemblies. Nat Commun 9:4122.

Claret M, Smith MA, Knauf C, Al-Qassab H, Woods A, Heslegrave A, Piipari K, Emmanuel JJ, Colom A, Valet P, Cani PD, Begum G, White A, Mucket P, Peters M, Mizuno K, Batterham RL, Giese KP, Ashworth A, Burcelin R, Ashford ML, Carling D, Withers DJ (2011). Deletion of Lkb1 in pro-opiomelanocortin neurons impairs peripheral glucose homeostasis in mice. Diabetes. 60:735-45.

Clift D, McEwan WA, Labzin LI, Konieczny V, Mogessie B, James LC, Schuh M (2017) A method for the acute and rapid degradation of endogenous proteins. Cell 172: 1692-1706.

Debanne D, Inglebert Y, Russier M (2019) Plasticity of intrinsic neuronal excitability. Curr Opin Neurobiol 54:73-82.

Duvarci S, Pare D (2014) Amygdala microcircuits controlling learned fear. Neuron 82:966-980.

Fei-Wang, Tian DR, Tso P, Han JS (2012) Diet-induced obese rats exhibit impaired LKB1-AMPK signaling in hypothalamus and adipose tissue. Peptides. 35:23-30.

Ferreira G, Miranda MI, De la Cruz V, Rodriguez-Ortiz CJ, Bermudez-Rattoni F. 2005. Basolateral amygdala glutamatergic activation enhances taste aversion through NMDA receptor activation in the insular cortex. The European journal of neuroscience 22: 2596-2604.

Ferreira G, Ferry B, Meurisse M, Levy F (2006) Forebrain structures specifically activated by conditioned taste aversion. Behav Neurosci 120:952-962.

819 Frankland PW, Josselyn SA, Anagnostaras SG, Kogan JH, Takahashi E, Silva AJ (2004)
820 Consolidation of CS and US representations in associative fear conditioning.
821 Hippocampus 14:557-569.
822 Frick A, Johnston D (2005) Plasticity of dendritic excitability. J Neurobiol 64:100-115.
823 Gal-Ben-Ari S, Kenney JW, Ounalla-Saad H, Taha E, David O, Levitan D, Gildish I, Panja
824 D, Pai B, Wibrand K, Simpson TI, Proud CG, Bramham CR, Armstrong JD,
825 Rosenblum K (2012) Consolidation and translation regulation. Learn Mem 19:410-
826 422.
827 Gallo M, Roldan G, Bures J. 1992. Differential involvement of gustatory insular cortex and
828 amygdala in the acquisition and retrieval of conditioned taste aversion in rats.
829 Behav Brain Res 52: 91-97.
830 Garcia-Delatorre P, Perez-Sanchez C, Guzman-Ramos K, Bermudez-Rattoni F (2014)
831 Role of glutamate receptors of central and basolateral amygdala nuclei on retrieval
832 and reconsolidation of taste aversive memory. Neurobiol Learn Mem 111:35-40.
833 Gore F, Schwartz EC, Brangers BC, Aladi S, Stujenske JM, Likhtik E, Russo MJ, Gordon
834 JA, Salzman CD, Axel R (2015) Neural Representations of Unconditioned Stimuli
835 in Basolateral Amygdala Mediate Innate and Learned Responses. Cell 162:134-
836 145.
837 Grossman SE, Fontanini A, Wieskopf JS, Katz DB. 2008. Learning-related plasticity of
838 temporal coding in simultaneously recorded amygdala-cortical ensembles. J
839 Neurosci 28: 2864-2873.
840 Grundemann J, Luthi A (2015) Ensemble coding in amygdala circuits for associative
841 learning. Curr Opin Neurobiol 35:200-206.
842 Haley MS, Fontanini A, Maffei A (2016) Laminar- and Target-Specific Amygdalar Inputs
843 in Rat Primary Gustatory Cortex. J Neurosci 36:2623-2637.
844 Hempel CM, Sugino K, Nelson SB (2007) A manual method for the purification of
845 fluorescently labeled neurons from the mammalian brain. Nat Protoc 2:2924-2929.
846 Hardie DG (2007) AMP-activated protein kinase as a drug target. Annu Rev Pharmacol
847 Toxicol 47:185-210.
848 Holtmaat A, Caroni P (2016) Functional and structural underpinnings of neuronal
849 assembly formation in learning. Nat Neurosci 19:1553-1562.
850 Hashikawa K, Naka M, Nakayama D, Matsumoto N, Neve R, Matsuki N (2013) Blockade
851 of stimulus convergence in amygdala neurons disrupts taste associative learning.
852 J Neurosci 33:4958-4963.
853 Inberg S, Jacob E, Elkobi A, Edry E, Rappaport A, Simpson TI, Armstrong JD, Shomron
854 N, Pasmanik-Chor M, Rosenblum K (2016) Fluid consumption and taste novelty
855 determines transcription temporal dynamics in the gustatory cortex. Mol Brain
856 9:13.
857 Johansen JP, Cain CK, Ostroff LE, LeDoux JE (2011) Molecular mechanisms of fear
858 learning and memory. Cell 147:509-524.
859 Josselyn SA, Kida S, Silva AJ (2004) Inducible repression of CREB function disrupts
860 amygdala-dependent memory. Neurobiol Learn Mem 82:159-163.
861 Kandel ER (2001) The molecular biology of memory storage: a dialogue between genes
862 and synapses. Science 294:1030-1038.
863 Kandel ER, Dudai Y, Mayford MR (2014) The molecular and systems biology of memory.
864 Cell 157:163-186

Katz DB, Simon SA, Nicolelis MA. 2001. Dynamic and multimodal responses of gustatory cortical neurons in awake rats. J Neurosci 21: 4478-4489.

Koh MT, Thiele TE, Bernstein IL (2002) Inhibition of protein kinase A activity interferes with long-term, but not short-term, memory of conditioned taste aversions. Behav Neurosci 116:1070-1074.

Koh MT, Clarke SN, Spray KJ, Thiele TE, Bernstein IL (2003) Conditioned taste aversion memory and c-Fos induction are disrupted in RIIbeta-protein kinase A mutant mice. Behav Brain Res 143:57-63.

Kwon SK, Sando R, 3rd, Lewis TL, Hirabayashi Y, Maximov A, Polleux F (2016) LKB1 Regulates Mitochondria-Dependent Presynaptic Calcium Clearance and Neurotransmitter Release Properties at Excitatory Synapses along Cortical Axons. PLoS Biol 14:e1002516.

Lamprecht R, Dudai Y (1996) Transient expression of c-Fos in rat amygdala during training is required for encoding conditioned taste aversion memory. Learn Mem 3:31-41.

Lavi K, Jacobson GA, Rosenblum K, Luthi A (2018) Encoding of Conditioned Taste Aversion in Cortico-Amygdala Circuits. Cell Rep 24:278-283.

Levitan D, Gal-Ben-Ari S, Heise C, Rosenberg T, Elkobi A, Inberg S, Sala C, Rosenblum K (2016a) The differential role of cortical protein synthesis in taste memory formation and persistence. NPJ Sci Learn 1:16001.

Levitan D, Fortis-Santiago Y, Figueroa JA, Reid EE, Yoshida T, Barry NC, Russo A, Katz DB. (2016b). Memory Retrieval Has a Dynamic Influence on the Maintenance Mechanisms That Are Sensitive to zeta-Inhibitory Peptide (ZIP). J Neurosci 36: 10654-10662.

Levitan D, Lin JY, Wachutka J, Mukherjee N, Nelson SB, Katz DB (2019) Single and population coding of taste in the gustatory cortex of awake mice. J Neurophysiol.

Li JX, Yoshida T, Monk KJ, Katz DB (2013) Lateral hypothalamus contains two types of palatability-related taste responses with distinct dynamics. J Neurosci. 33: 9462-73.

Lin JY, Reilly S (2012) Amygdala-gustatory insular cortex connections and taste neophobia. Behav Brain Res 235:182-188.

Lin JY, Arthurs J, Reilly S (2018) The effects of amygdala and cortical inactivation on taste neophobia. Neurobiol Learn Mem 155:322-329.

Lizcano JM, Goransson O, Toth R, Deak M, Morrice NA, Boudeau J, Hawley SA, Udd L, Makela TP, Hardie DG, Alessi DR (2004) LKB1 is a master kinase that activates 13 kinases of the AMPK subfamily, including MARK/PAR-1. EMBO J 23:833-843.

Ma L, Wang DD, Zhang TY, Yu H, Wang Y, Huang SH, Lee FS, Chen ZY (2011) Region-specific involvement of BDNF secretion and synthesis in conditioned taste aversion memory formation. J Neurosci 31:2079-2090.

Maffei A, Haley M, Fontanini A (2012) Neural processing of gustatory information in insular circuits. Curr Opin Neurobiol 22:709-716.

Matthies H (1989) In search of cellular mechanisms of memory. Prog Neurobiol 32:277-349.

Mayford M, Reijmers L (2015) Exploring Memory Representations with Activity-Based Genetics. Cold Spring Harb Perspect Biol 8:a021832.

910 Momcilovic M, Shackelford DB (2015) Targeting LKB1 in cancer - exposing and exploiting
911 vulnerabilities. Br J Cancer 113:574-584.
912 Molero-Chamizo A, Rivera-Urbina GN (2017) Effects of lesions in different nuclei of the
913 amygdala on conditioned taste aversion. Exp Brain Res 235:3517-3526.
914 Motanis H, Maroun M, Barkai E (2014) Learning-induced bidirectional plasticity of intrinsic
915 neuronal excitability reflects the valence of the outcome. Cereb Cortex 24:1075-
916 1087.
917 Nakada D, Saunders TL, Morrison SJ (2010) Lkb1 regulates cell cycle and energy
918 metabolism in haematopoietic stem cells. Nature 468:653-658.
919 Mozzachiodi R, Byrne JH (2010) More than synaptic plasticity: role of nonsynaptic
920 plasticity in learning and memory. Trends Neurosci 33:17-26.
921 Navarro M, Spray KJ, Cubero I, Thiele TE, Bernstein IL. 2000a. cFos induction during
922 conditioned taste aversion expression varies with aversion strength. Brain Res
923 887: 450-453.
924 Nelson SB, Sugino K, Hempel CM (2006) The problem of neuronal cell types: a
925 physiological genomics approach. Trends Neurosci 29:339-345.
926 Neseliler S, Narayanan D, Fortis-Santiago Y, Katz D, Birren S. 2011. Genetically Induced
927 Cholinergic Hyper-Innervation Enhances Taste Learning. Frontiers in Systems
928 Neuroscience 5.
929 Piette CE, Baez-Santiago MA, Reid EE, Katz DB, Moran A. 2012. Inactivation of
930 basolateral amygdala specifically eliminates palatability-related information in
931 cortical sensory responses. J Neurosci 32: 9981-9991.
932 Pignatelli M, Ryan TJ, Roy DS, Lovett C, Smith LM, Muralidhar S, Tonegawa S (2019)
933 Engram Cell Excitability State Determines the Efficacy of Memory Retrieval.
934 Neuron 101:274-284 e275.
935 Rappaport AN, Jacob E, Sharma V, Inberg S, Elkobi A, Ounallah-Saad H, Pasmanik-
936 Chor M, Edry E, Rosenblum K (2015) Expression of Quinone Reductase-2 in the
937 Cortex Is a Muscarinic Acetylcholine Receptor-Dependent Memory Consolidation
938 Constraint. J Neurosci 35:15568-15581.
939 Ryan TJ, Roy DS, Pignatelli M, Arons A, Tonegawa S (2015) Memory. Engram cells retain
940 memory under retrograde amnesia. Science 348:1007-1013.
941 Reijmers LG, Perkins BL, Matsuo N, Mayford M (2007) Localization of a stable neural
942 correlate of associative memory. Science 317:1230-1233.
943 Sadacca BF, Rothwax JT, Katz DB. 2012. Sodium concentration coding gives way to
944 evaluative coding in cortex and amygdala. J Neurosci 32: 9999-10011.
945 Samuel MA, Voinescu PE, Lilley BN, de Cabo R, Foretz M, Viollet B, Pawlyk B, Sandberg
946 MA, Vavvas DG, Sanes JR (2014) LKB1 and AMPK regulate synaptic remodeling
947 in old age. Nat Neurosci 17:1190-1197.
948 Samuelsen CL, Gardner MP, Fontanini A (2012) Effects of cue-triggered expectation on
949 cortical processing of taste. Neuron 74:410-422.
950 Shelly M, Cancedda L, Heilshorn S, Sumbre G, Poo MM (2007) LKB1/STRAD promotes
951 axon initiation during neuronal polarization. Cell 129:565-577.
952 Shackelford DB, Shaw RJ (2009) The LKB1-AMPK pathway: metabolism and growth
953 control in tumour suppression. Nat Rev Cancer 9:563-575.

954 Shima Y, Sugino K, Hempel CM, Shima M, Taneja P, Bullis JB, Mehta S, Lois C, Nelson
955 SB (2016) A Mammalian enhancer trap resource for discovering and manipulating
956 neuronal cell types. Elife 5:e13503.
957 Soto A, Gasalla P, Begega A, Lopez M. 2017. c-Fos activity in the insular cortex, nucleus
958 accumbens and basolateral amygdala following the intraperitoneal injection of
959 saccharin and lithium chloride. Neurosci Lett 647: 32-37.
960 Samuelsen CL, Gardner MP, Fontanini A (2012) Effects of cue-triggered expectation on
961 cortical processing of taste. Neuron 74:410-422.
962 Spiegel I, Mardinly AR, Gabel HW, Bazinet JE, Couch CH, Tzeng CP, Harmin DA,
963 Greenberg ME (2014) Npas4 regulates excitatory-inhibitory balance within neural
964 circuits through cell-type-specific gene programs. Cell 157:1216-1229.
965 Stevens CF (1996) Spatial learning and memory: the beginning of a dream. Cell 87:1147-
966 1148.
967 Stuber GD, Sparta DR, Stamatakis AM, van Leeuwen WA, Hardjoprajitno JE, Cho S, Tye
968 KM, Kempadoo KA, Zhang F, Deisseroth K, Bonci A (2011) Excitatory
969 transmission from the amygdala to nucleus accumbens facilitates reward seeking.
970 Nature 475:377-380.
971 Titley HK, Brunel N, Hansel C (2017) Toward a Neurocentric View of Learning. Neuron
972 95:19-32.
973 Trapnell C, Roberts A, Goff L, Pertea G, Kim D, Kelley DR, Pimentel H, Salzberg SL, Rinn
974 JL, Pachter L (2012) Differential gene and transcript expression analysis of RNA-
975 seq experiments with TopHat and Cufflinks. Nat Protoc 7:562-578.
976 Tye KM, Prakash R, Kim SY, Fenno LE, Grosenick L, Zarabi H, Thompson KR, Gradinaru
977 V, Ramakrishnan C, Deisseroth K (2011) Amygdala circuitry mediating reversible
978 and bidirectional control of anxiety. Nature 471:358-362.
979 Shima Y, Sugino K, Hempel CM, Shima M, Taneja P, Bullis JB, Mehta S, Lois C, Nelson
980 SB (2016) A Mammalian enhancer trap resource for discovering and manipulating
981 neuronal cell types. Elife 5:e13503.
982 Sugino K, Hempel CM, Miller MN, Hattox AM, Shapiro P, Wu C, Huang ZJ, Nelson SB
983 (2006) Molecular taxonomy of major neuronal classes in the adult mouse forebrain.
984 Nat Neurosci 9:99-107.
985 Tonegawa S, Pignatelli M, Roy DS, Ryan TJ (2015) Memory engram storage and
986 retrieval. Curr Opin Neurobiol 35:101-109.
987 Uematsu A, Kitamura A, Iwatsuki K, Uneyama H, Tsurugizawa T. 2015. Correlation
988 Between Activation of the Prelimbic Cortex, Basolateral Amygdala, and Agranular
989 Insular Cortex During Taste Memory Formation. Cereb Cortex 25: 2719-2728.
990 Xi P, Du J, Liang H, Han J, Wu Z, Wang H, He L, Wang Q, Ge H, Li Y, Xue J, Tian D
991 (2018) Intraventricular Injection of LKB1 Inhibits the Formation of Diet-Induced
992 Obesity in Rats by Activating the AMPK-POMC Neurons-Sympathetic Nervous
993 System Axis. Cell Physiol Biochem. 47:54-66.
994 Yassin L, Benedetti BL, Jouhanneau JS, Wen JA, Poulet JF, Barth AL (2010) An
995 embedded subnetwork of highly active neurons in the neocortex. Neuron 68:1043-
996 1050.
997 Yasoshima Y, Sako N, Senba E, Yamamoto T. 2006. Acute suppression, but not chronic
998 genetic deficiency, of c-fos gene expression impairs long-term memory in aversive
999 taste learning. Proc Natl Acad Sci U S A 103: 7106-7111.

Zhang J, Zhang D, McQuade JS, Behbehani M, Tsien JZ, Xu M (2002) c-fos regulates neuronal excitability and survival. Nat Genet 30:416-420.

Zhang W, Linden DJ (2003) The other side of the engram: experience-driven changes in neuronal intrinsic excitability. Nat Rev Neurosci 4:885-900.

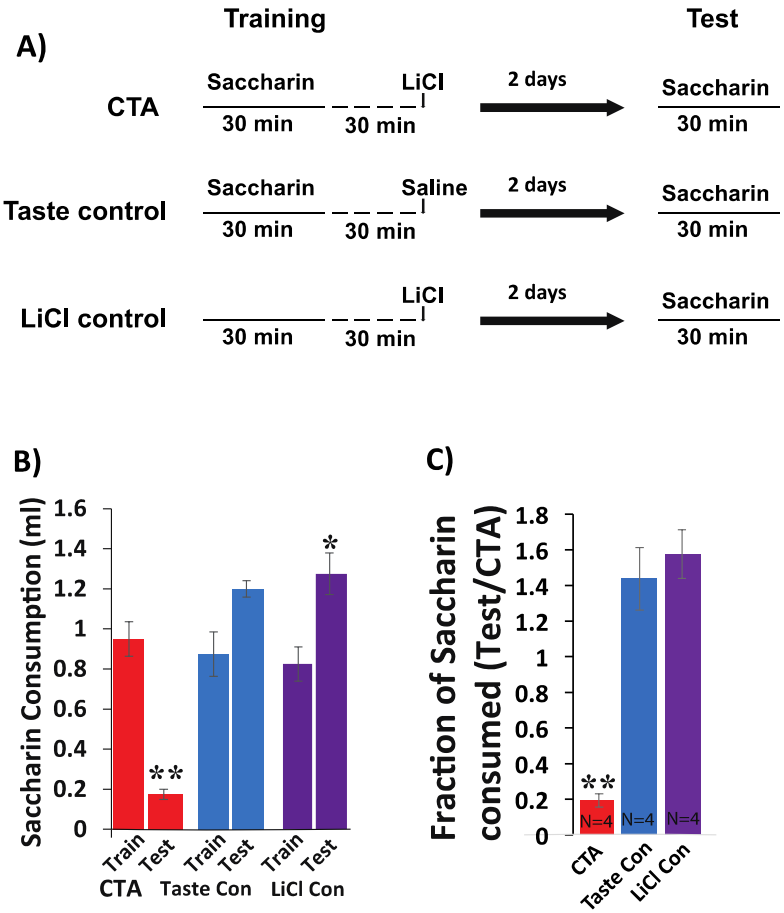

Figure 1-figure supplement 1. Testing CTA in mice. (**A**) Time line showing behavioral paradigm. CTA and Taste control receive 30 min of 0.5% saccharin consumption followed by intraperitoneal injection (I.P) injection of lithium-chloride (LiCl; 0.15 M, 2% body-weigh) or saline 30 min later. The lithium control group receives the same I.P injection of LiCl, but no saline during the training phase. All groups were tested for consumption of saccharin during 30 min exposure 48 hours later. (**B**) Saccharin consumption decreases following LiCl-induced malaise (N=4/group). There was main effect on drinking volume of saccharin between the groups across sessions: f(4,18)=28.63, p=1E-7 A subsequent pairwise comparison between training and test revealed p=4E-5 for CTA group, p=0.016 for LiCl group and p=0.172 for taste group. (**C**) Measuring CTA memory strength. The strength of CTA memory was determined by quantifying the fraction of saccharin consumption in the test day out of the consumption in the training day. Comparing CTA strength of all groups revealed main effect for difference between groups f(2,9)=34.08, p=6E-5; p=2.5E-4 for CTA vs taste control and p=0.00011 for CTA vs LiCl control and p=1 for taste control vs LiCl control (On way ANOVA with Bonferroni correction). *p<0.05; **p<0.01.labeled neurons from the BLA in the YFP-H mouse line (Feng et al., 2000; Sugino et al., 2006; Jasnow et al., 2013; McCullough et al., 2016) which expresses YFP under the Thy1 promoter in a large population of excitatory projection neurons located in the anterior part of the nucleus.

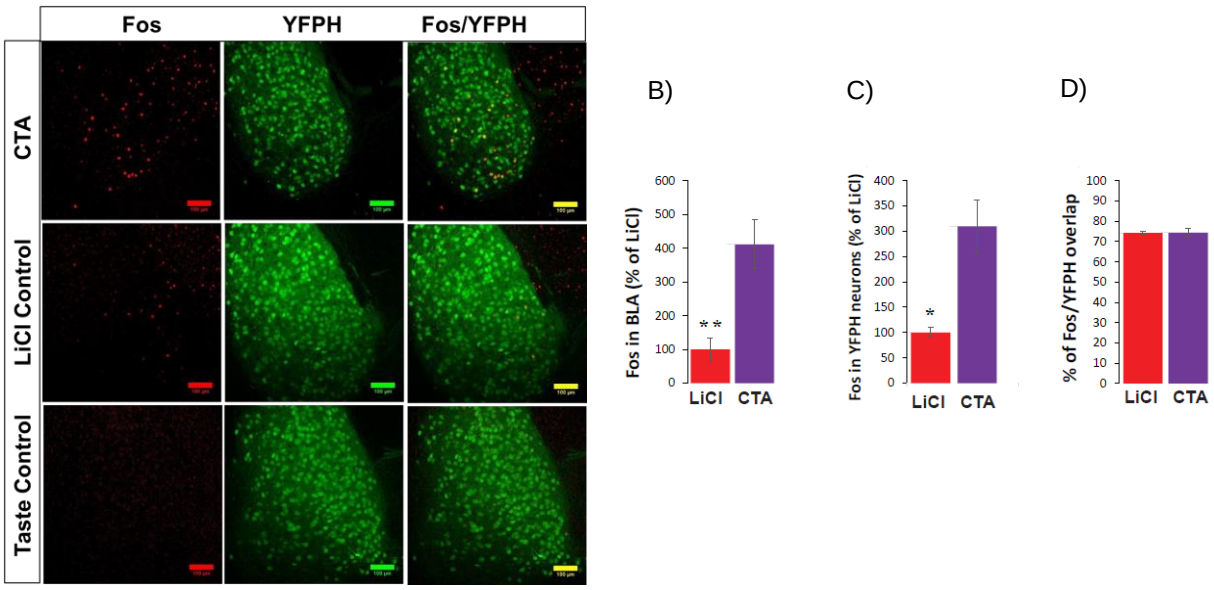

Figure 2-figure supplement 1. CTA increases Fos protein expression in BLApn including those in strain YFP-H. (**A**) Images of YFP$^+$ neurons in the BLA (green) and Fos protein (red) 4 hours following CTA training, LiCl and taste controls. Note that the taste control group has no Fos$^+$ signal and so is not shown in B-D. (**B**) CTA increased Fos expression in BLA relative to the LiCl and taste controls (F(2,11)=21.2; p=4E-4; Post hoc (Bonferroni corrected) difference between CTA and LiCl groups: p=0.003, and p=4E-4 between CTA and taste control groups, N=4/group). (**C**) As in (B), but only for Fos overlapping YFP expression (f(2,11)=23.5: p=0.008, post hoc: CTA and taste control groups: p=4E-4; N=3-4/group). *p<0.05; **p<0.01. (**D**) In both CTA and LiCl control conditions the expression of Fos protein was similarly localized to YFP$^+$ neurons (74.4% for CTA and 74.2% for LiCl control).

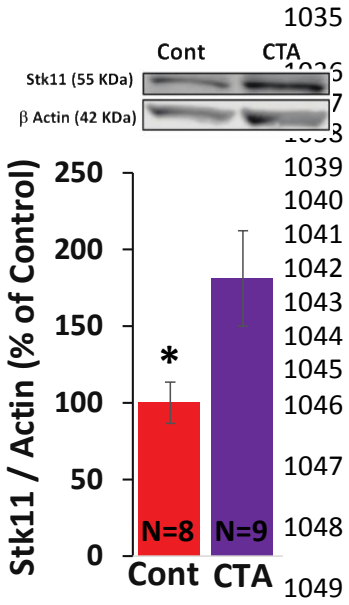

Figure 2-figure supplement 2. Stk11 protein expression following CTA training. YFP-H mice were trained for CTA or received a taste control and 4 hours later the anterior BLA (guided by YFP expression) was subdissected and used for immunoblotting with antibodies raised against Stk11 and actin (as loading control). CTA increased the expression of Stk11 (t(15)=2.28; p=0.037, N=8/9 per group). *p<0.05.

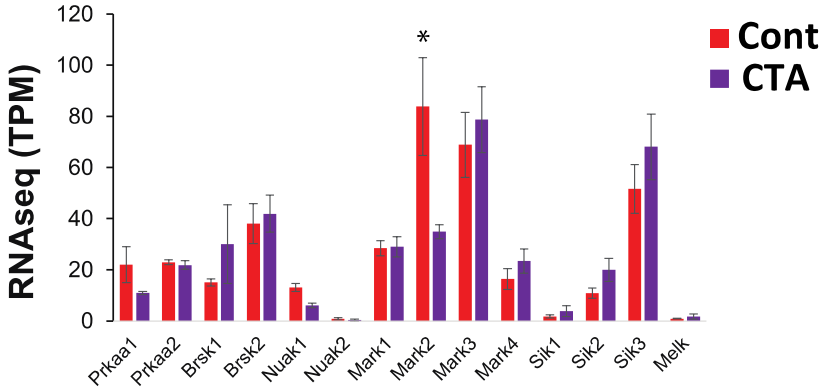

Figure 2-figure supplement 3. BLApn transcript levels of known downstream substrates of Stk11, the members of the AMP-related kinase family (Lizcano et al., 2004). RNA sequencing from BLApn 4 hours following CTA training. Note that Mark2 mRNA expression is reduced in taste control mice relative CTA trained mice (N=4/group; *p<0.05); TPM- transcripts per million.

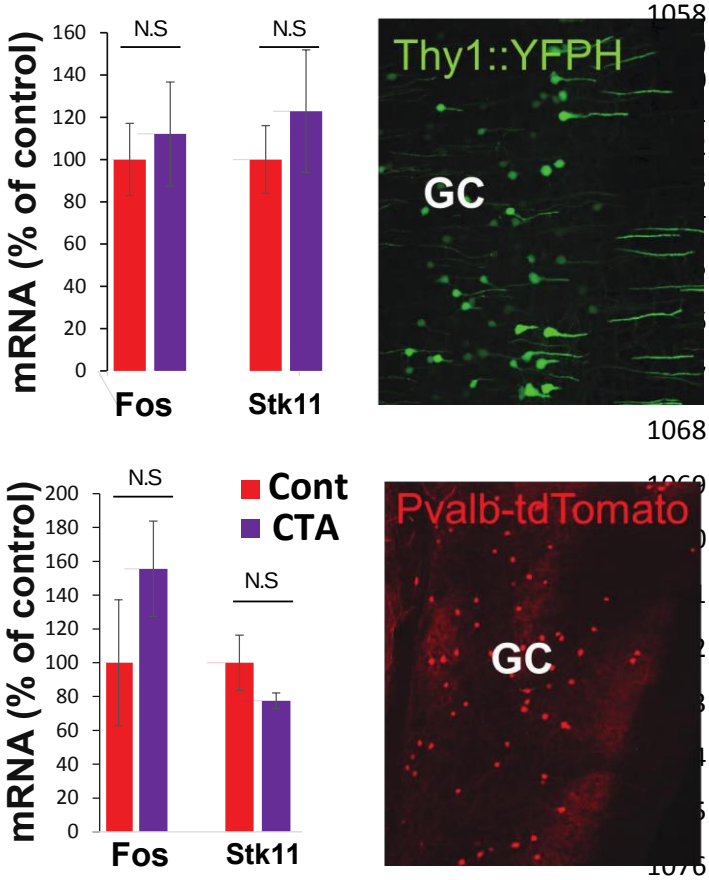

Figure 2-figure supplement 4. RNA sequencing from GC. Top. YFP-H L5 pyramidal neurons and Pvalb-tdTomato positive interneurons in the GC. Fos and Stk11 did not differ significantly between CTA and taste control groups.

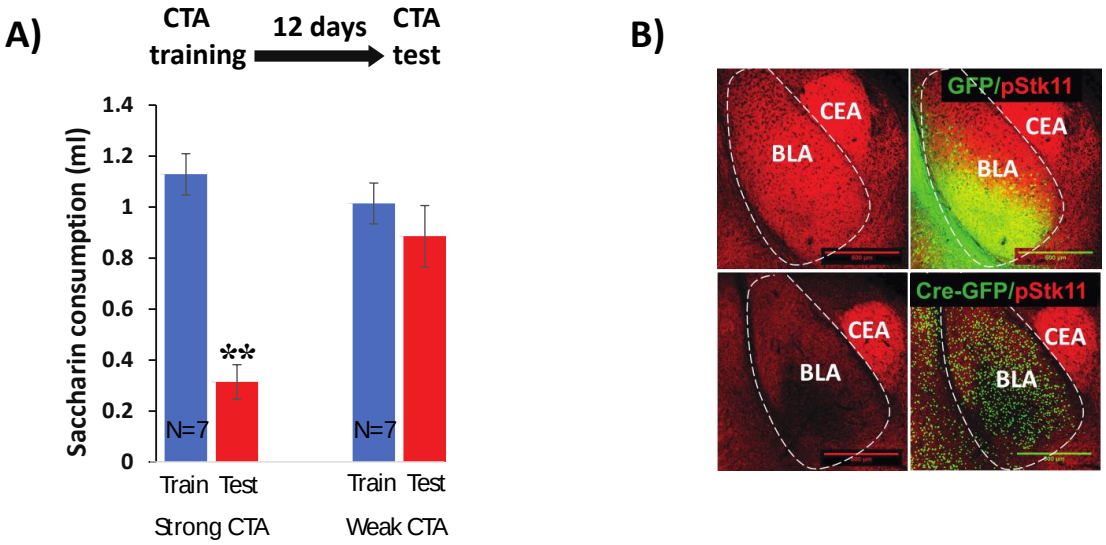

Figure 4-figure supplement 1. (**A**) CTA elicited by a dose of 0.15 M LiCl 1% body weight (Weak CTA) does not last 12 days following training (N=7, t(12)=0.89, p=0.391). On the other hand CTA elicited by a LiCl dose of 0.15M 2% body weight (Strong CTA) does (N=7, t(12)=7.757; p=5.15E-06). (**B**) Conditional knock-out of Stk11 reduces phospho-Stk11 protein expression. Immunostaining for Stk11 protein (phosphorylated at serine 431) was performed 10 days after BLA infection with Cre or control viruses. Scale bar: 500 µm.

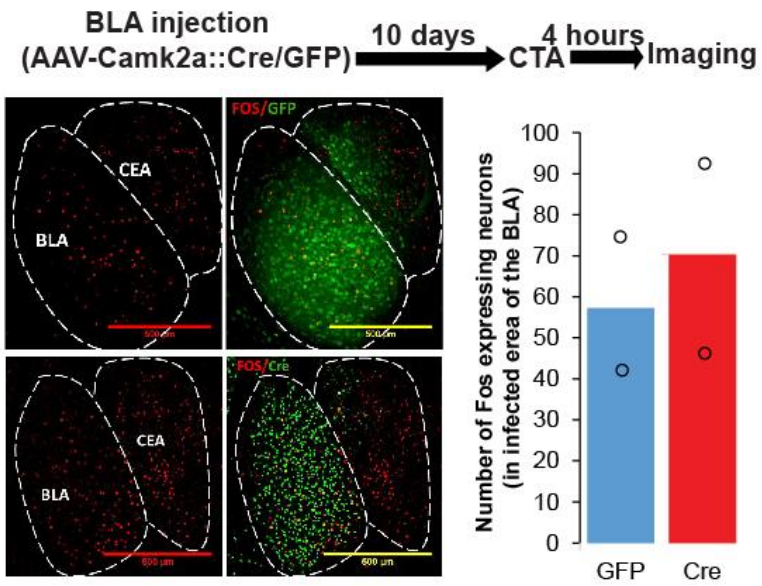

Figure 5- figure supplement 1. CTA induced Fos protein expression persists after Stk11 deletion in BLApn. Fos protein expression in the BLA was measured 4 hours following CTA training in Stk11$^{f/f}$ receiving Cre or control virus injection 10 days earlier.

Table 1. Transcripts in YFP$^+$ BLApn with significantly altered expression 4 hours following CTA. Criteria: 2 ≤ fold change ≤ 0.5, p<0.01, TPM > 30 (TPM=transcript per million).

Symbol	Fold-Change	P-Value	Gene name
Upregulated in CTA vs taste control			
Nptx1	2.02	1.57E-4	Neuronal pentraxin 1
Ric8	2.06	0.0017	RIC8 guanine nucleotide exchange factor A
Mmab	3.66	0.0019	methylmalonic aciduria (cobalamin deficiency) cblB type homolog
1110008F13Rik	2.08	0.0028	RAB5 interacting factor
Kbtbd4	2.09	0.0044	kelch repeat and BTB (POZ) domain containing 4(Kbtbd4)
Nudt21	2.14	0.0077	nudix (nucleoside diphosphate linked moiety X)-type motif 21
Fos	2.64	0.0094	FBJ osteosarcoma oncogene
Magoh	2.72	0.0095	mago homolog, exon junction complex core component
Downregulated in CTA vs taste control			
Surf2	0.40	5.42E-4	surfeit gene 2(Surf2)
Tmem136	0.39	8.69E-4	transmembrane protein 136
Stk11	0.50	0.0011	serine/threonine kinase 11(Stk11)
Kank3	0.28	0.0022	KN motif and ankyrin repeat domains 3
Lrrn1	0.49	0.0024	leucine rich repeat protein 1, neuronal
Trpc1	0.48	0.0032	transient receptor potential cation channel, subfamily C, memb. 1
Prpf6	0.49	0.0045	pre-mRNA splicing factor 6
Tctex1d2	0.49	0.0052	Tctex1 domain containing 2
Gpr108	0.37	0.0056	G protein-coupled receptor 108
Vkorc1	0.39	0.0069	vitamin K epoxide reductase complex, subunit 1
D10Wsu102e	0.50	0.0082	DNA segment, Chr 10, Wayne State University 102, expressed
Tmem107	0.28	0.0089	transmembrane protein 107

Table 2. Transcripts in YFP$^+$ L5 pyramidal neurons in the GC with significantly altered expression 4 hours following CTA. Criteria: 2 ≤ fold change ≤ 0.5, p<0.01, TPM > 30.

Gene Symbol	Fold-Change	P-Value	Gene name
			Transcript Down-regulated CTA vs taste control
Exosc1	0.43	0.008	exosome component 1

Table 3. Transcripts in Pvalb^{+} interneurons in the GC with significant altered expression 4 hours following CTA. Criteria: 2 ≤ fold change ≤ 0.5, p<0.01, TPM > 30.

Symbol	Fold-Change	P-Value	Gene name
Upregulated in CTA vs taste control			
Uprt	3.38	0.001	uracil phosphoribosyltransferase
Snca	2.66	0.001	synuclein, alpha
1810043H04Rik	2.57	0.004	NADH:ubiquinone oxidoreductase complex Assemb.Fact. 8
Dedd	2.47	0.001	death effector domain-containing
Fam149b	2.26	0.007	family with sequence similarity 149, member B
Jazf1	2.12	0.008	JAZF zinc finger 1
Nup54	2.09	0.007	nucleoporin 54
Downregulated in CTA vs taste control			
Dear1	0.006	0.0006	dual endothelin 1/angiotensin II receptor 1
Nt5c3b	0.20	0.002	5'-nucleotidase, cytosolic IIIB
Lrrc16b	0.26	0.010	capping protein regulator and myosin 1 linker 3
Enc1	0.31	0.005	ectodermal-neural cortex 1
Asap2	0.38	0.004	ArfGAP with SH3 domain, ankyrin repeat and PH domain 2
Pacs2	0.38	0.0002	phosphofurin acidic cluster sorting protein 2
Ncan	0.42	0.008	neurocan
uc008jhl.1	0.42	0.010	
Smarcd3	0.45	0.006	SWI/SNF Related, Matrix Assoc.Actin Dep.Reg. Chromatin, Subfamily D, Member 3
Tbce	0.46	0.002	tubulin-specific chaperone E
uc009mzt.1	0.47	0.008	
Anxa6	0.50	0.001	annexin A6

Table 4. Electrophysiological properties of BLApn: Stk11 knockout vs. GFP controls.

Group	Statistics	Resting membrane potential (mV)	Access resistance (mΩ)	Input Resistance (mΩ)	mAHP (mV)	sAHP (mV)	Action potential Amplitude (mV)	Action potential half width (ms)	Action potential threshold (mV)	Sag ratio
KO	mean	-78.23	19.68	105.33	7.44	0.92	74.41	0.80	-50.01	0.13
	S.D.	3.73	2.76	24.88	1.93	0.35	6.58	0.10	2.44	0.04
GFP	mean	-76.96	18.02	85.41	9.71	0.64	78.05	0.79	-48.30	0.15
	S.D.	2.66	3.47	17.65	1.64	0.26	4.39	0.07	2.55	0.03
	F	2.59	4.47	14.41	26.69	13.78	7.17	0.19	7.68	7.48
	p	0.112	0.0383	3.29E-4	2.54E-06	4.32E-4	0.0094	0.664	0.0073	0.008

Table 5. Electrophysiological properties of BLApn: Fos knockout vs. GFP controls.

Group	Statistics	Resting membrane potential (mV)	Access resistance (mΩ)	Input Resistance (mΩ)	mAHP (mV)	sAHP (mV)	Action potential Amplitude (mV)	Action potential half width (ms)	Action potential threshold (mV)
KO	mean	-75.43	19.63	113.91	10.34	0.40	65.87	0.72	-40.79
	S.D.	5.08	4.95	27.73	4.30	0.19	8.31	0.11	5.83
GFP	mean	-76.50	14.35	86.01	8.95	0.38	73.30	0.74	-45.62
	S.D.	3.38	5.17	19.58	2.05	0.17	5.11	0.12	3.02
	F	0.768	13.882	16.812	2.096	0.144	14.334	0.224	13.306
	p	0.385	5.04E-04	1.55E-04	0.154	0.706	4.18E-04	0.638	6.40E-04